PNAS
www.pnas.org

Supplementary Information for

Maximizing the value of forest restoration for tropical mammals by detecting three-dimensional habitat associations

Nicolas J. Deere, Gurutzeta Guillera-Arroita, Tom Swinfield, David T. Milodowski, David A. Coomes, Henry Bernard, Glen Reynolds, Zoe G. Davies and Matthew J. Struebig

Corresponding author: Nicolas J. Deere
Email: n.j.deere@kent.ac.uk

This PDF file includes:

www.pnas.org/cgi/doi/10.1073/pnas.2001823117

S1.1: Developing three-dimensional LiDAR metrics

The method we employed to estimate the vertical profile of leaf area from LiDAR point clouds is based on a simple one-dimensional Beer-Lambert approximation of light propagation through a turbid medium, (e.g. 1, 2, 3), which has been validated against directly harvested foliage profiles in tropical forests in both the Brazilian Amazon (2) and Costa Rica (3). This model assumes a laterally homogeneous canopy, with a vertical distribution of plant density described by the function, PAD(*z*), where *z* is the depth into the canopy from its top. The rate at which propagating ray traces are intersected by vegetation is proportional to PAD(*z*):

$$\frac{d\emptyset(z)}{dz} = -\kappa PAD(z)\emptyset(z)$$

where $\Phi(z)$ is a function describing the probability that a ray penetrates to a canopy depth *z* without prior interception, and κ is a correction factor that accounts for canopy features, such as the leaf angle distribution, that modulate this relationship. Integrating this equation over a canopy layer of thickness Δz, then approximating $\Phi(z=x)$ as the ratio of pulses that penetrate to a depth $z=x$ before intercepting vegetation, $n(z \leq x)$, to the total number of pulses *n* yields:

$$PAD_{M1a,i} = \frac{1}{\kappa \Delta z} ln\left(\frac{\sum_{z_i=0}^{z_i=z} n_{i,k=1}}{\sum_{z=0}^{z=z2} n_{i,k=1}}\right)$$

The numerator in the log-term defines the number of returns entering the top of a canopy layer; the denominator defines the number of returns penetrating through the canopy layer into the underlying layers. We consider only the first point of contact for each LiDAR pulse within the canopy, which closely mimics the field sampling approach

published by MacArthur and Horn (4). Representing the canopy as a series of layers, it is thus possible to estimate the vertical distribution of vegetation within the canopy. In order to produce these profiles, the point cloud is aggregated at a horizontal resolution of 20-m. The lowermost 2-m of the canopy is not considered.

From the estimated canopy profiles, we derived four of the metrics used in the subsequent analysis:

- Plant area index: the total intercepting plant area in the canopy, calculated by integrating *PAD(z)* over the full canopy profile.

  $$Plant\ area\ index = \sum_{i=1}^{N} PAD_i$$

  This provides a first order measure of the density of the vegetation, although is also correlated with canopy height in this forest (5).

- Structural diversity index: describes the range of niches available within the canopy. It increases both with the number of canopy layers (canopy height) with vegetation, and as PAD is more evenly distributed between the canopy layers.

  $$Structural\ diversity\ index = \sum_{i=1}^{N} PAD_i ln(PAD_i)$$

  This has previously been used with regards to related canopy structure to tropical forest dynamics (2).

- Shape: a morphological parameter that describes the relative distribution of material within the canopy (6), here calculated as the ratio of the height in the canopy with the highest PAD to the height of the 99th percentile of the PAD distribution.

- Number of contiguous canopy layers: calculated as the number of canopy layers based on regions of continuous PAD – essentially mimicking the field process of counting canopy layers (e.g. Clark et al., 2008). Layer continuity is defined based on contiguous regions with PAD greater than a threshold value of 0.1 m^2m^{-3}.

S1.2: Bayesian linear model specification

As a preliminary assessment of the structural signature of forest degradation, we employed a series of Bayesian linear models to determine differences in forest canopy properties across categorical degradation classes. Linear models were implemented in the statistical software JAGS (Just Another Gibbs Sampler) version 4.3.0 (7), called through R using the package "jagsUI" (6). Uninformative priors were used throughout, incorporating flat normal and wide uniform priors for intercept/slope and variance parameters respectively. We specified three Markov chains per parameter, each comprising 12,000 iterations thinned by a factor of 10, 2,000 of which were discarded during the burn-in period. Convergence was assessed visually, to determine adequate mixing of chains, and statistically, using the Gelman-Rubin statistic, with values <1.1 indicating convergence (8). Model fit was assessed using a predictive posterior check, which compares the observed data against a simulated, idealized dataset (9). We extracted Bayesian *P* values as a numerical summary of the posterior predictive distribution, with values of 0.5 indicating adequate model fit.

S2.1: Occupancy model description

Our model formulation employed single-species models as analytical building blocks (10). Within a traditional single-season, single-species framework, occupancy is estimated at defined locations using spatially or temporally replicated samples to account for imperfect detection (11). Here, we extend this to incorporate spatial and temporal replication and multi-species inference. Our framework comprises three conditionally-dependent sub-components describing the partially observed processes of occupancy (*z*), habitat use (*a*) (state process models) and detection (observation model). These sub-models correspond to the hierarchical nature of our sampling design, equivalent to sampling location, camera trap station (spatial replicate) and survey (temporal replicate) respectively. We modelled occurrence, *z*, of species *i* at sampling location *j* as the realization of Bernoulli trial:

$$z_{i,j} \sim Bernoulli(\psi_{i,j})$$

where $z_{i,j}$ is a binary variable indicating species presence/absence and $\psi_{i,j}$ expresses the probability of species occurrence at a given sampling location. Habitat use, α, of species *i* within sampling location *j* at camera trap station *l*, is defined as the outcome of a second Bernoulli process conditional on species presence, $z_{i,j}$:

$$a_{i,j,l}|z_{i,j} \sim Bernoulli(z_{i,j} \cdot \vartheta_{i,j,l})$$

where $a_{i,j,l}$ is a binary variable indicating presence/absence at the camera trap station and ϑ expresses the probability-of-use. To account for imperfect detection in habitat use, we specified a third Bernoulli process:

$$y_{i,j,l,k}|a_{i,j,l} \sim Bernoulli(a_{i,j,l,k} \cdot p_{i,j,l,k})$$

where $y_{i,j,l,k}$ represents a four-dimensional array containing the observed detection/non-detection data, *k* is the temporal replicate and $p_{i,j,l,k}$ is the detection

probability conditional on species presence. Under this formulation we interpret model parameters as: (1) the probability that a sampling location lies within the home range of at least one individual of a given species relative to coarse-scale structural covariates describing home range characteristics; (2) the probability that a camera trap station is preferentially selected to meet ecological demands relative to fine-scale structural properties given that the sampling location is represented in the home range, and, (3) the probability of detecting a mammal species during a survey replicate given that the camera trap station was being utilized.

Prior to modelling, detection/non-detection data for each camera trap were binned into independent sampling occasions of six-days in length (2-7 replicates per site). We excluded three species with fewer than five detections throughout sampling (banded linsang, *Prionodon linsang*; banteng, *Bos javanicus*; smooth-coated otter, *Lutrogale perspicillata*), as models are unable to discern changes in occupancy from those in detection when observations are very sparse (12). We also acknowledge that strictly arboreal species (i.e. gibbons, *Hylobates* sp., langurs, *Presbytis sp.*, small-toothed palm civets, *Arctogalidia trivirgata*) cannot be reliably monitored using our sampling design and restrict inference to terrestrial/semi-arboreal species.

Multi-scale occupancy models assume independence between spatial replicates (13), however, spatially clustered designs may result in Markovian dependence as a result of animal ranging behavior (14). To test this assumption, we employed a Jaccard Index (*J*), to determine the degree of similarity in detection histories between camera stations nested within sites for all study species (15). We found little evidence of similarity, with the exception of the bearded pig (J=0.51; P=0.008), Bornean yellow muntjac (J=0.33; 0.015),

red muntjac (J=0.27; P=0.048) and pig-tailed macaque (J=0.31; 0.008), for which correspondence was attributed to high levels of abundance.

Single-species models were linked by an additional hierarchical component that modelled species-specific parameters as realizations from a community-level distribution. This approach assumes species respond similarly, but not identically, to environmental conditions. Species-specific parameter estimates thus reflect a compromise between individual response and the average response of the community, modulated by detection history. This process induces shrinkage (the borrowing of statistical strength by individual species across the community), which has been shown to improve estimation precision for data-poor species infrequently detected during sampling (16).

Hierarchical multi-species occupancy models were implemented using a Bayesian framework, specified with uninformative priors for intercept and slope parameters. We modelled variance parameters associated with temporal random effects hierarchically using a half-Cauchy distribution to mitigate potential overestimation due to few factor levels (17). We specified three Markov chains per parameter, each comprising 150,000 iterations with a thin rate of 100 and a burn-in period of 50,000. Convergence was inspected visually to determine adequate mixing of chains, and using the Gelman-Rubin statistic, with values <1.1 indicating convergence (9). Model fit was quantified using a predictive posterior check, which compares the observed data against a simulated, idealized dataset (9). We extracted Bayesian P values as a numerical summary of the posterior predictive distribution, with values of 0.5 indicating adequate model fit. We assessed model fit using a Pearson χ^2 discrepancy measure for binomial data and a "lack of fit" statistic (18) (Table S2).

To determine optimal spatial extents for structural covariates, we implemented scale optimization methods proposed by McGarigal et al. (19), which have been shown to improve the predictive performance of statistical models. We constructed 126 multi-scale multi-species occupancy models to compare structural covariates aggregated across a range of buffer radii (occupancy covariates: 1-2 km, *N*=3; probability-of-use covariates: 10-500 m, *N*=7). The best-supported spatial extent for each structural covariate was identified by ranking models according to WAIC (Watanabe Akaike-Information-Criterion; Table S2).

S2.2: Model code

We provide model code for the hierarchical Bayesian multi-species, multi-scale occupancy model, written in the BUGS language and implemented in JAGS called through R.

```
model {
  # Hyper-priors for occupancy, habitat use and detection intercepts
  #==========================================
  mu.alpha.psi ~ dnorm(0, 0.01)
  sigma.alpha.psi ~ dunif(0, 10)
  tau.alpha.psi <- pow(sigma.alpha.psi, -2)

  mu.alpha.theta ~ dnorm(0, 0.01)
  sigma.alpha.theta ~ dunif(0, 10)
  tau.alpha.theta <- pow(sigma.alpha.theta, -2)

  mu.alpha.p ~ dnorm(0, 0.01)
  sigma.alpha.p ~ dunif(0, 10)
  tau.alpha.p <- pow(sigma.alpha.p, -2)

  # Hyper-priors for occupancy, habitat use and detection covariate coefficients
  #=====================================================
  mu.beta1.psi ~ dnorm(0, 0.01)
  sigma.beta1.psi ~ dunif(0, 10)
  tau.beta1.psi <- pow(sigma.beta1.psi, -2)

  mu.beta2.psi ~ dnorm(0, 0.01)
  sigma.beta2.psi ~ dunif(0, 10)
```

```
tau.beta2.psi <- pow(sigma.beta2.psi, -2)

mu.beta1.theta ~ dnorm(0, 0.01)
sigma.beta1.theta ~ dunif(0, 10)
tau.beta1.theta <- pow(sigma.beta1.theta, -2)

mu.beta2.theta ~ dnorm(0, 0.01)
sigma.beta2.theta ~ dunif(0, 10)
tau.beta2.theta <- pow(sigma.beta2.theta, -2)

mu.beta1.p ~ dnorm(0, 0.01)
sigma.beta1.p ~ dunif(0, 10)
tau.beta1.p <- pow(sigma.beta1.p, -2)

mu.beta2.p ~ dnorm(0, 0.01)
sigma.beta2.p ~ dunif(0, 10)
tau.beta2.p <- pow(sigma.beta2.p, -2)

mu.beta3.p ~ dnorm(0, 0.01)
sigma.beta3.p ~ dunif(0, 10)
tau.beta3.p <- pow(sigma.beta3.p, -2)

# Hyperprior for half-Cauchy scale parameter for occupancy and habitat use models
#=========================================================
xi.sd.psi ~ dunif(0, 10)
xi.tau.psi <- pow(xi.sd.psi, -2)
xi.sd.theta ~ dunif(0, 10)
xi.tau.theta <- pow(xi.sd.theta, -2)

# Species-specific parameters drawn as realisations from the community distributions
#=========================================================
for(i in 1:n.sp){
   alpha.psi[i] ~ dnorm(mu.alpha.psi, tau.alpha.psi)
   alpha.theta[i] ~ dnorm(mu.alpha.theta, tau.alpha.theta)
   alpha.p[i] ~ dnorm(mu.alpha.p, tau.alpha.p)

   beta1.psi[i] ~ dnorm(mu.beta1.psi, tau.beta1.psi)
   beta2.psi[i] ~ dnorm(mu.beta2.psi, tau.beta2.psi)
   beta1.theta[i] ~ dnorm(mu.beta1.theta, tau.beta1.theta)
   beta2.theta[i] ~ dnorm(mu.beta2.theta, tau.beta2.theta)
   beta1.p[i] ~ dnorm(mu.beta1.p, tau.beta1.p)
   beta2.p[i] ~ dnorm(mu.beta2.p, tau.beta2.p)
   beta3.p[i] ~ dnorm(mu.beta3.p, tau.beta3.p)
   }
```

```
# Hyperpriors/priors for temporal random effect
#==================================
for(i in 1:n.sp){
   # Random year effects for psi component
   for(year in 1:n.year){
      eps.psi[year, i] ~ dnorm(0, eps.tau.psi[i])
      eps.theta[year, i] ~ dnorm(0, eps.tau.theta[i])
      }

   eps.tau.psi[i] ~ dgamma(0.5, 0.5)
   xi.psi[i] ~ dnorm(0, xi.tau.psi)
   sigma.cauchy.psi[i] <- abs(xi.psi[i]) / sqrt(eps.tau.psi[i])

   eps.tau.theta[i] ~ dgamma(0.5, 0.5)
   xi.theta[i] ~ dnorm(0, xi.tau.theta)
   sigma.cauchy.theta[i] <- abs(xi.theta[i]) / sqrt(eps.tau.theta[i])
   }

# Ecological model for occurrence of species i in site j
#=======================================
for(i in 1:n.sp){
   for(j in 1:n.sites){
      logit(psi[j,i]) <- alpha.psi[i] + beta1.psi[i]*ForCov[j] + beta2.psi[i]*CH_SD.psi[j]
                         + xi.psi[i]*eps.psi[year.counter.psi[j],i]
      z[j,i] ~ dbern(psi[j,i])

# Sub-unit model, occurrence of species i within spatial replicate l
      for(l in 1:n.spatial[j]){
         logit(theta[j,l,i]) <- alpha.theta[i] + beta1.theta[i]*Structure1[j,l] +
                                beta2.theta[i]*Structure2[j,l] +
                                xi.theta[i]*eps.theta[year.counter.theta[j,l],i]
         mu.a[j,l,i] <- z[j,i] * theta[j,l,i]
         a[j,l,i] ~ dbern(mu.a[j,l,i])

# Detection model for replicated detection/non-detection observations
         for(k in 1:n.temporal[j,l]){
            logit(p[j,l,k,i]) <- alpha.p[i] + beta1.p[i]*PAI_Herb.p[j,l] +
                                 beta2.p[i]*Nlay.p[j,l] +  beta3.p[i]*TrapEffort[j,l]
            mu.p[j,l,k,i] <- a[j,l,i] * p[j,l,k,i]
            y[j,l,k,i] ~ dbern(mu.p[j,l,k,i])

# Calculate Pearson's Chi-squared residuals to assess goodness of fit
# Based on Kery and Royle: Applied hierarchical modelling in ecology, pp. 235
# Calculate the observed and expected residuals
# Add small value to prevent division by zero
```

```
#================================
            y.sim[j,l,k,i] ~ dbern(mu.p[j,l,k,i])
            chi2.obs[j,l,k,i] <- pow(y[j,l,k,i] - mu.p[j,l,k,i], 2)/ (mu.p[j,l,k,i] + 0.0001)
            chi2.sim[j,l,k,i] <- pow(y.sim[j,l,k,i] - mu.p[j,l,k,i], 2)/ (mu.p[j,l,k,i] +
                                 0.0001)
         }
         chi2.obs.sum[j,l,i] <- sum(chi2.obs[j,l,1:n.temporal[j,l],i])
         chi2.sim.sum[j,l,i] <- sum(chi2.sim[j,l,1:n.temporal[j,l],i])
      }
      chi2.obs.sum2[j,i] <- sum(chi2.obs.sum[j,1:n.spatial[j],i])
      chi2.sim.sum2[j,i] <- sum(chi2.sim.sum[j,1:n.spatial[j],i])
   }

# Calculate chi-squared discrepancy for each species
#====================================
   fit.sp.obs[i] <- sum(chi2.obs.sum2[,i])
   fit.sp.sim[i] <- sum(chi2.sim.sum2[,i])
   c.hat.sp[i] <- fit.sp.obs[i]/fit.sp.sim[i]
   bpv.sp[i] <- step(fit.sp.sim[i] - fit.sp.obs[i])
}

# Calculate model discrepancy measure and fit statistics
#=======================================
fit.obs <- sum(chi2.obs.sum2[1:n.sites, 1:n.sp])
fit.sim <- sum(chi2.sim.sum2[1:n.sites, 1:n.sp])
c.hat <- fit.obs/fit.sim
bpv <- step(fit.sim - fit.obs)

# Derived quantities
# Number of occupied sites
#==================
for(i in 1:n.sp) {
   Nocc.fs[i] <- sum(z[,i])
   }
```

```
 # Number of species occurring at each site
   #============================
   for(j in 1:n.sites) {
      Nsite[j] <- sum(z[j,])
      }
}
```

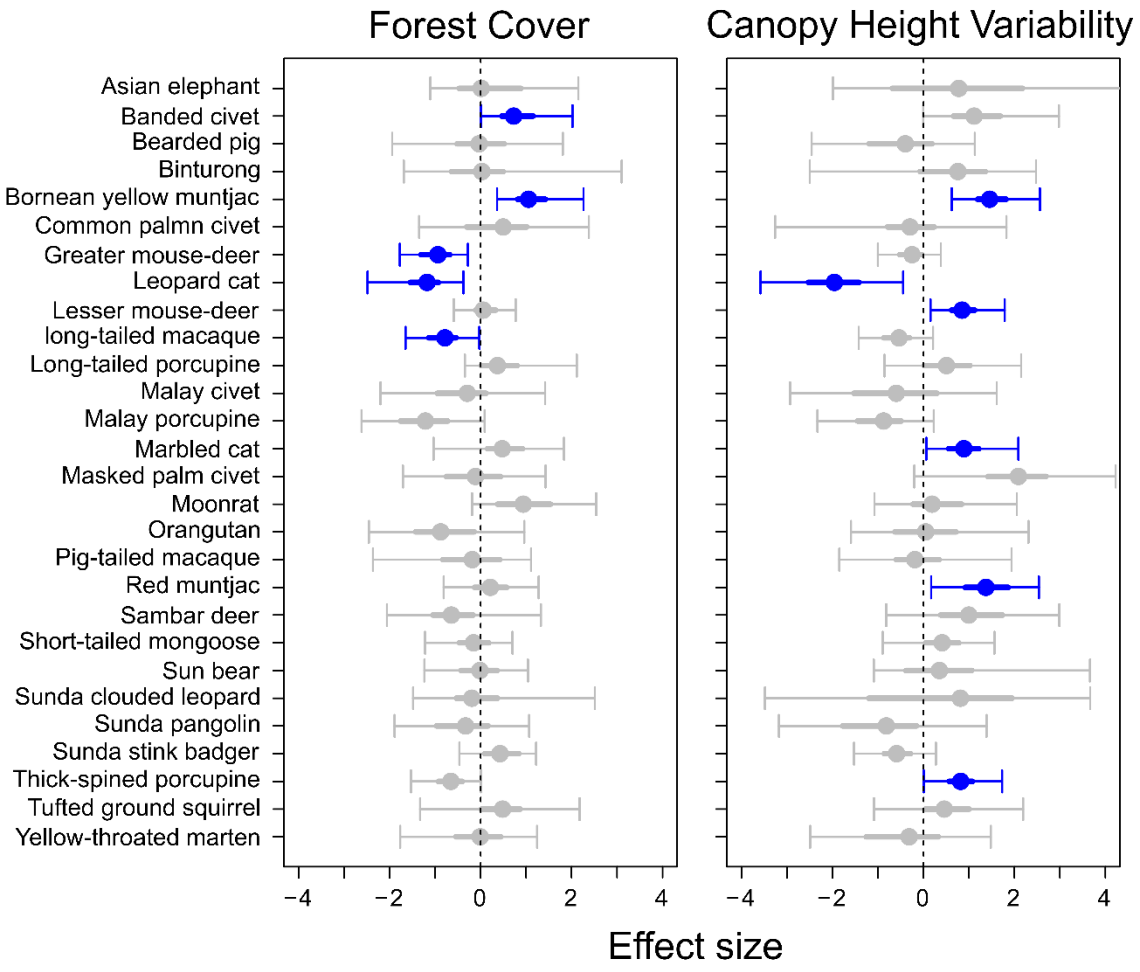

Figure S1: Landscape context factors influencing Bornean mammal occupancy. Covariates describe the (a) extent (forest cover) and (b) quality (canopy height variability) of forest habitat. Effect sizes are presented as posterior means (points) and 95% Bayesian credible intervals (BCI). Effects were considered substantial if the 95% BCI did not overlap zero (vertical dashed line). Responsive species are presented in blue.

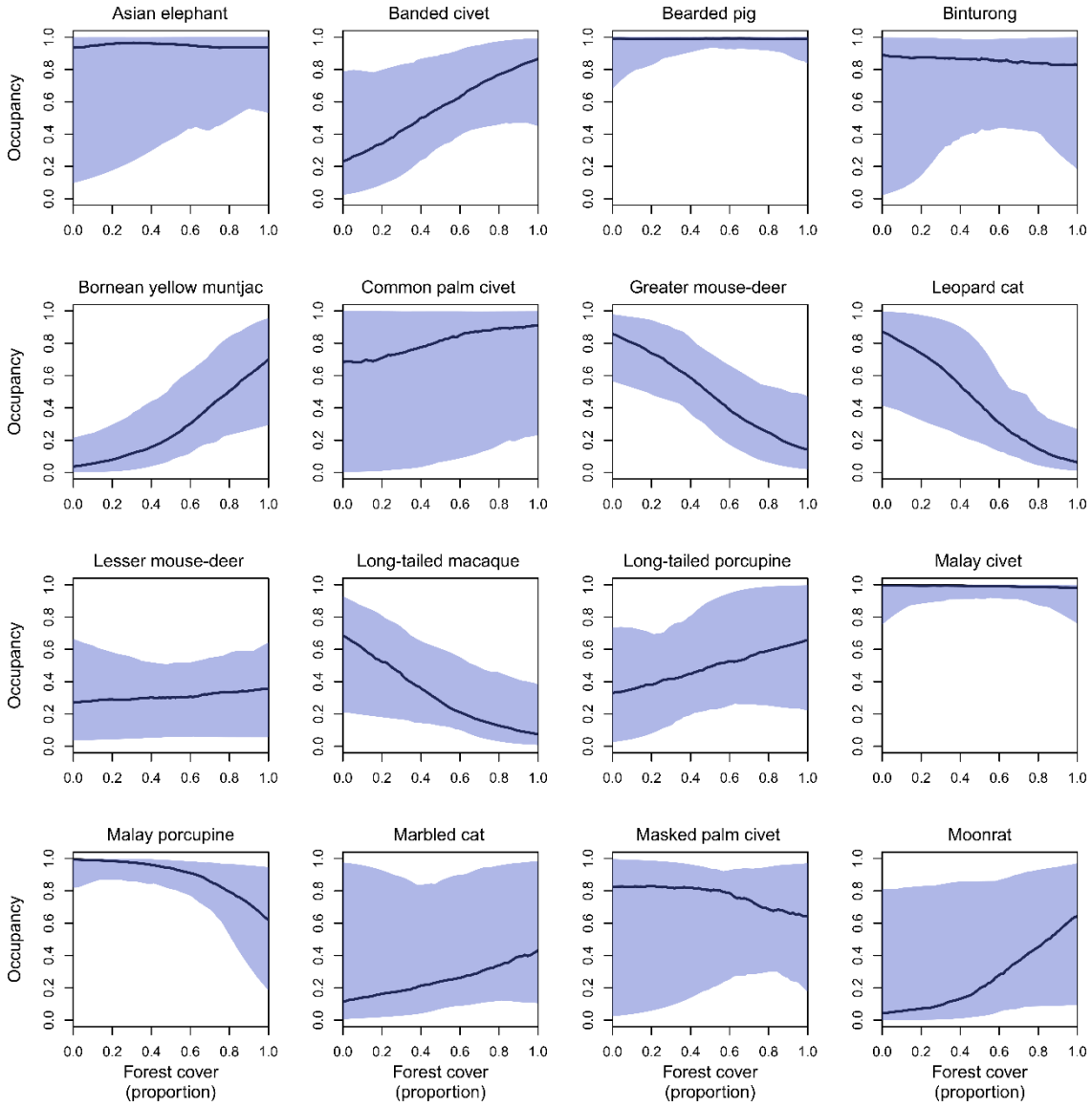
Asian elephant
Banded civet
Bearded pig
Binturong
Bornean yellow muntjac
Common palm civet
Greater mouse-deer
Leopard cat
Lesser mouse-deer
Long-tailed macaque
Long-tailed porcupine
Malay civet
Malay porcupine
Marbled cat
Masked palm civet
Moonrat
Occupancy
Forest cover (proportion)
0.0 0.2 0.4 0.6 0.8 1.0

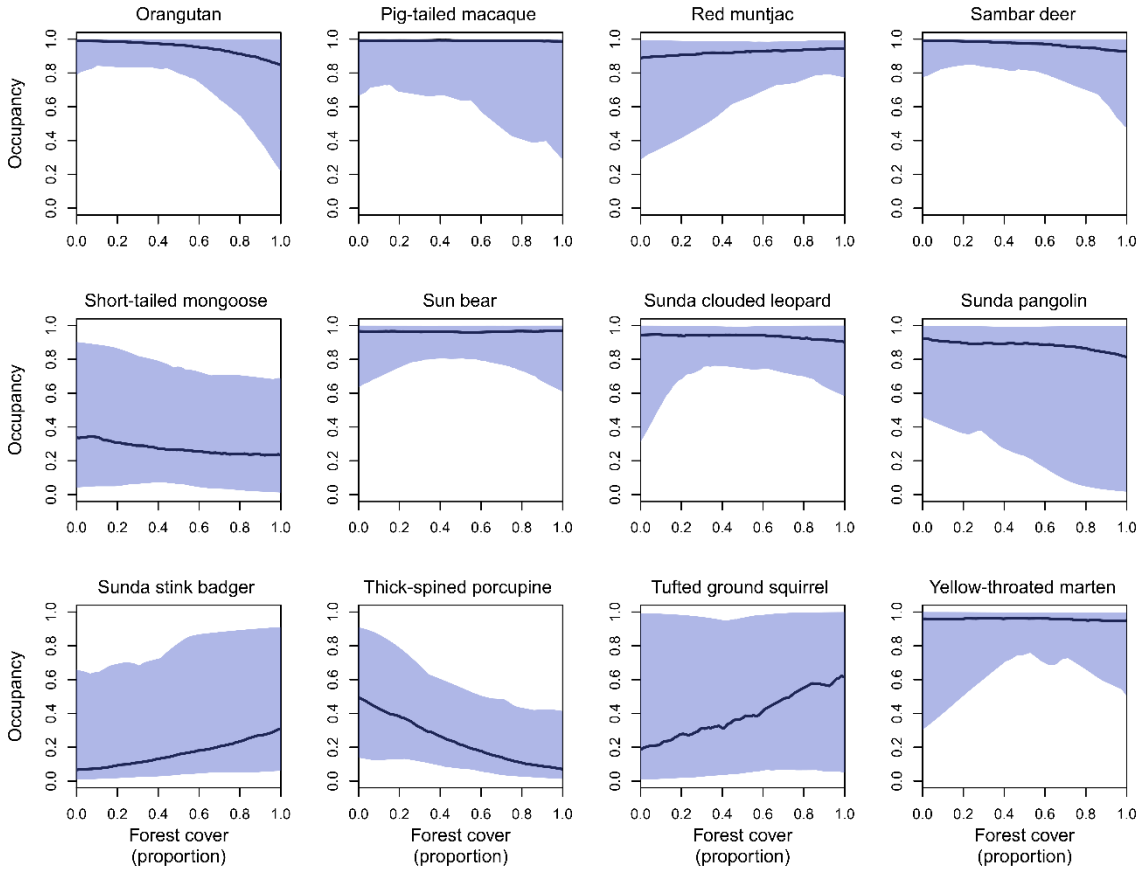

Figure S2: Occupancy relative to forest cover. Outputs are presented for the 28 medium-large terrestrial mammals encountered during sampling. Predicted posterior mean distribution values are presented in dark blue, while uncertainty, as indicated using 95% Bayesian credible intervals is visualized in light blue.

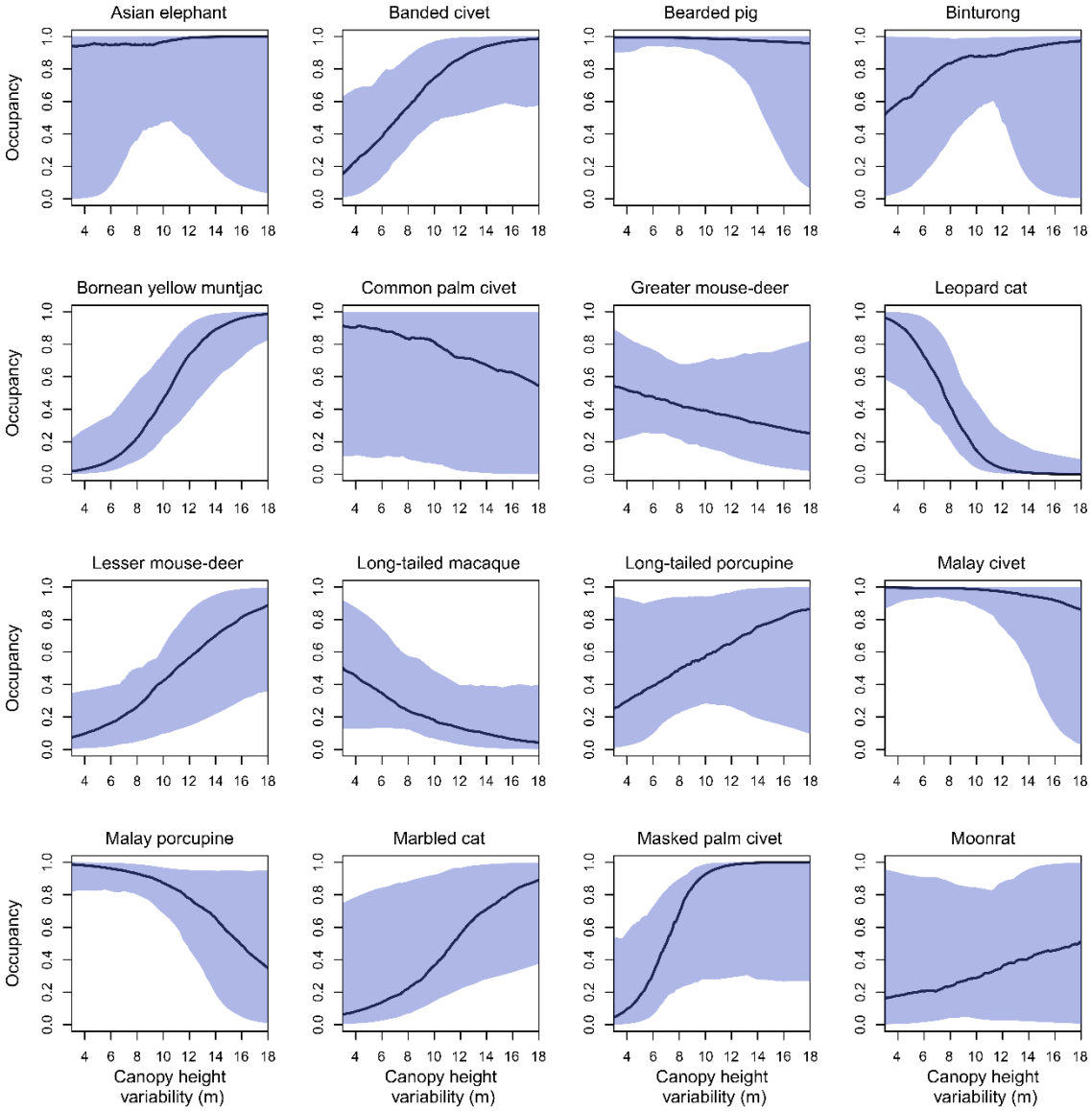
Asian elephant
Banded civet
Bearded pig
Binturong
Bornean yellow muntjac
Common palm civet
Greater mouse-deer
Leopard cat
Lesser mouse-deer
Long-tailed macaque
Long-tailed porcupine
Malay civet
Malay porcupine
Marbled cat
Masked palm civet
Moonrat
Occupancy
0.0 0.2 0.4 0.6 0.8 1.0
4 6 8 10 12 14 16 18
Canopy height variability (m)

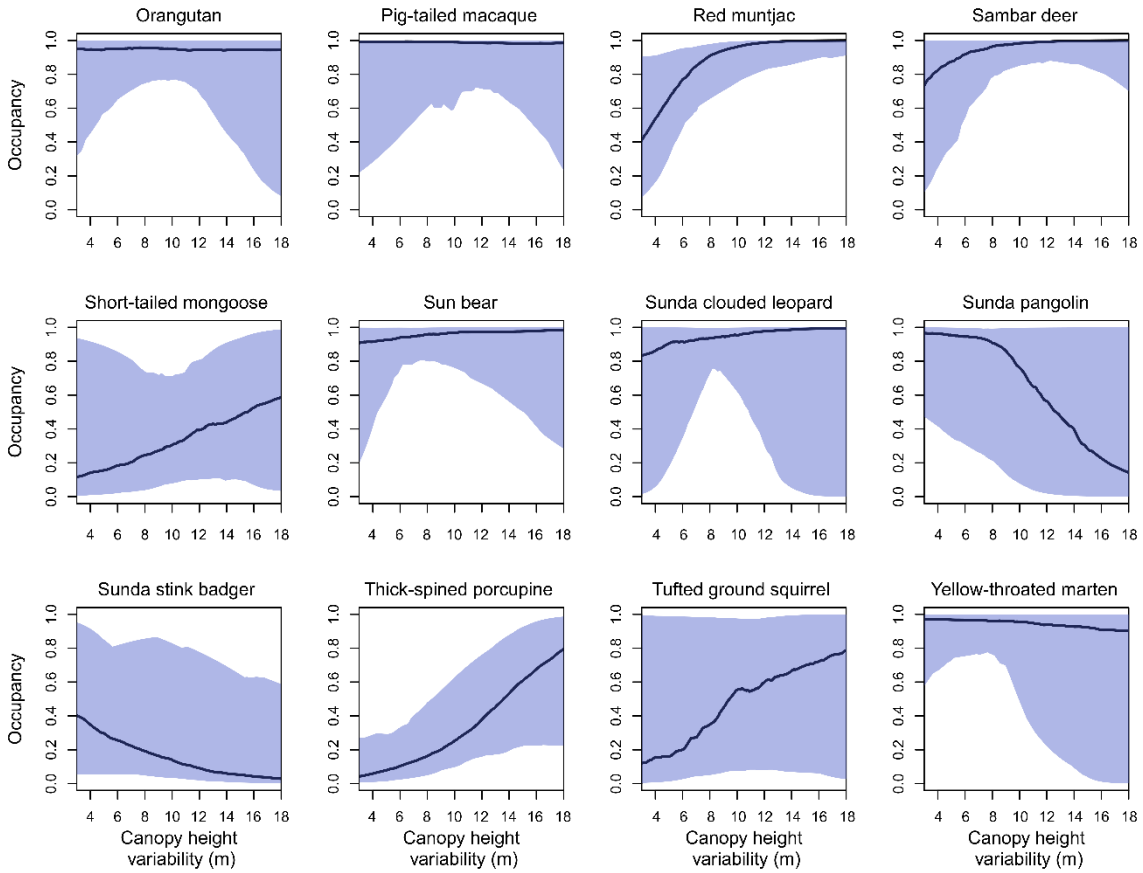

Figure S3: Occupancy relative to forest quality. Forest quality was defined using canopy height variability (m), with greater variability indicating better quality forest habitat. Outputs are presented for the 28 medium-large terrestrial mammals encountered during sampling. Predicted posterior mean distribution values are presented in dark blue, while uncertainty, as indicated using 95% Bayesian credible intervals is visualized in light blue.

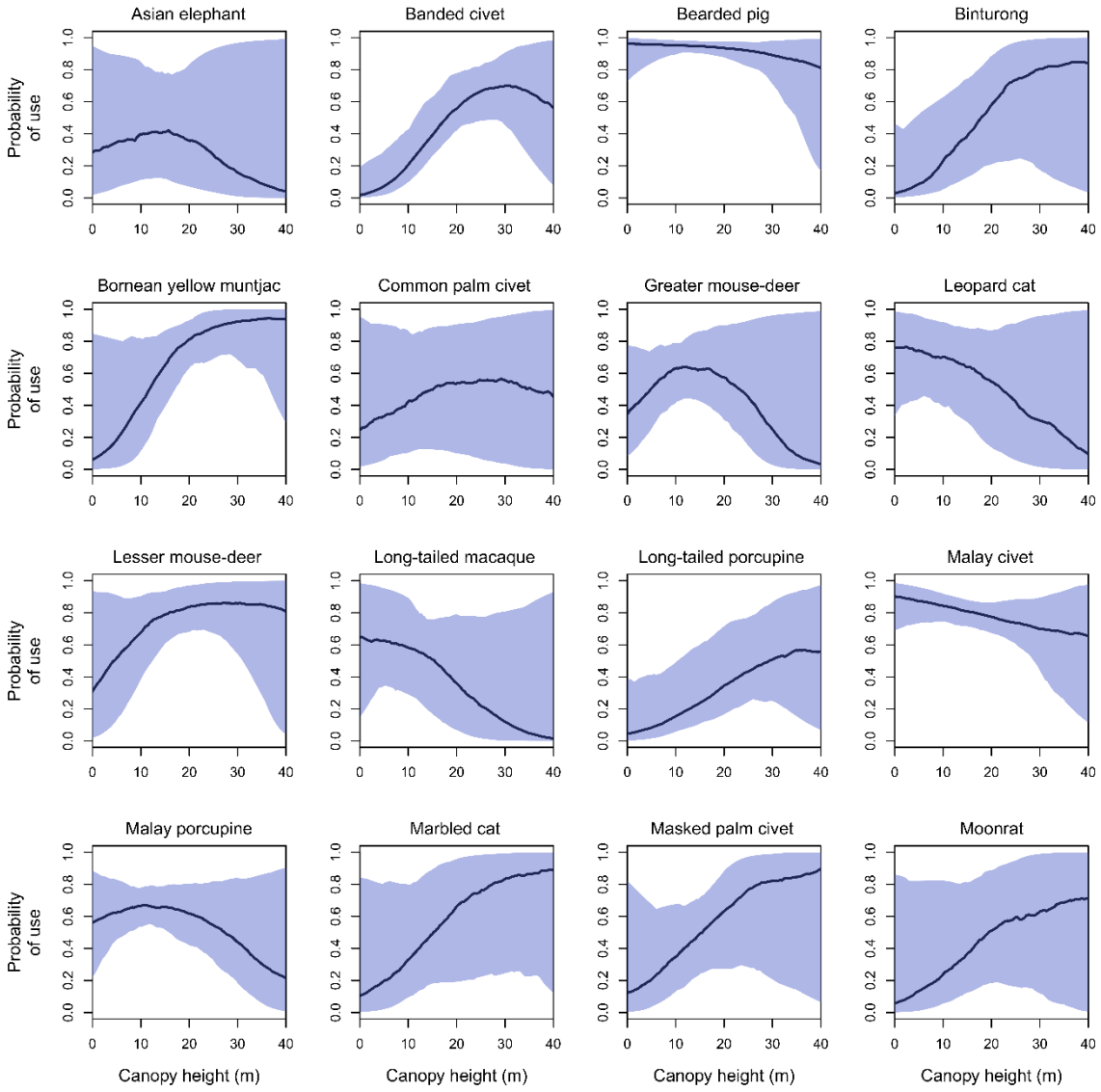
Asian elephant
Banded civet
Bearded pig
Binturong
Bornean yellow muntjac
Common palm civet
Greater mouse-deer
Leopard cat
Lesser mouse-deer
Long-tailed macaque
Long-tailed porcupine
Malay civet
Malay porcupine
Marbled cat
Masked palm civet
Moonrat
Probability of use
Canopy height (m)
0.0
0.2
0.4
0.6
0.8
1.0
0
10
20
30
40

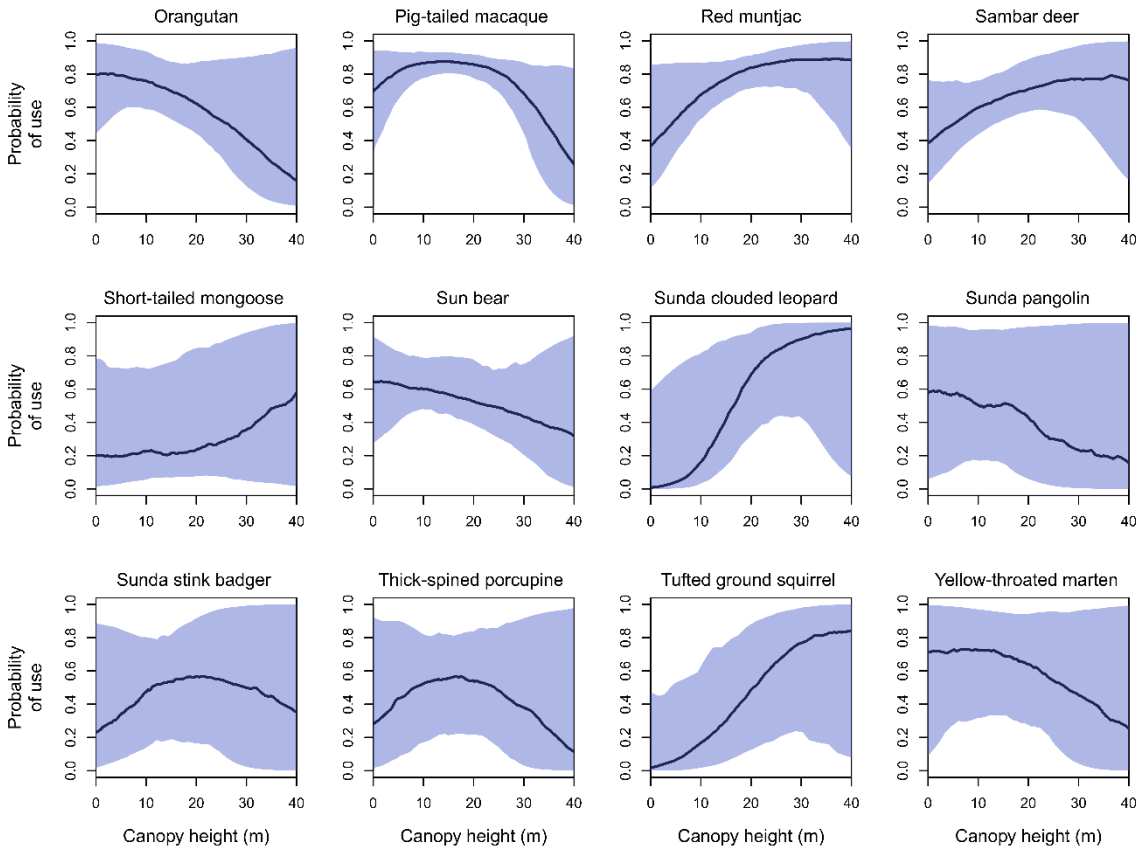

Figure S4: Probability-of-use relative to canopy height (m). Outputs are presented for the 28 medium-large terrestrial mammals encountered during sampling. Predicted posterior mean distribution values are presented in dark blue, while uncertainty, as indicated using 95% Bayesian credible intervals is visualized in light blue.

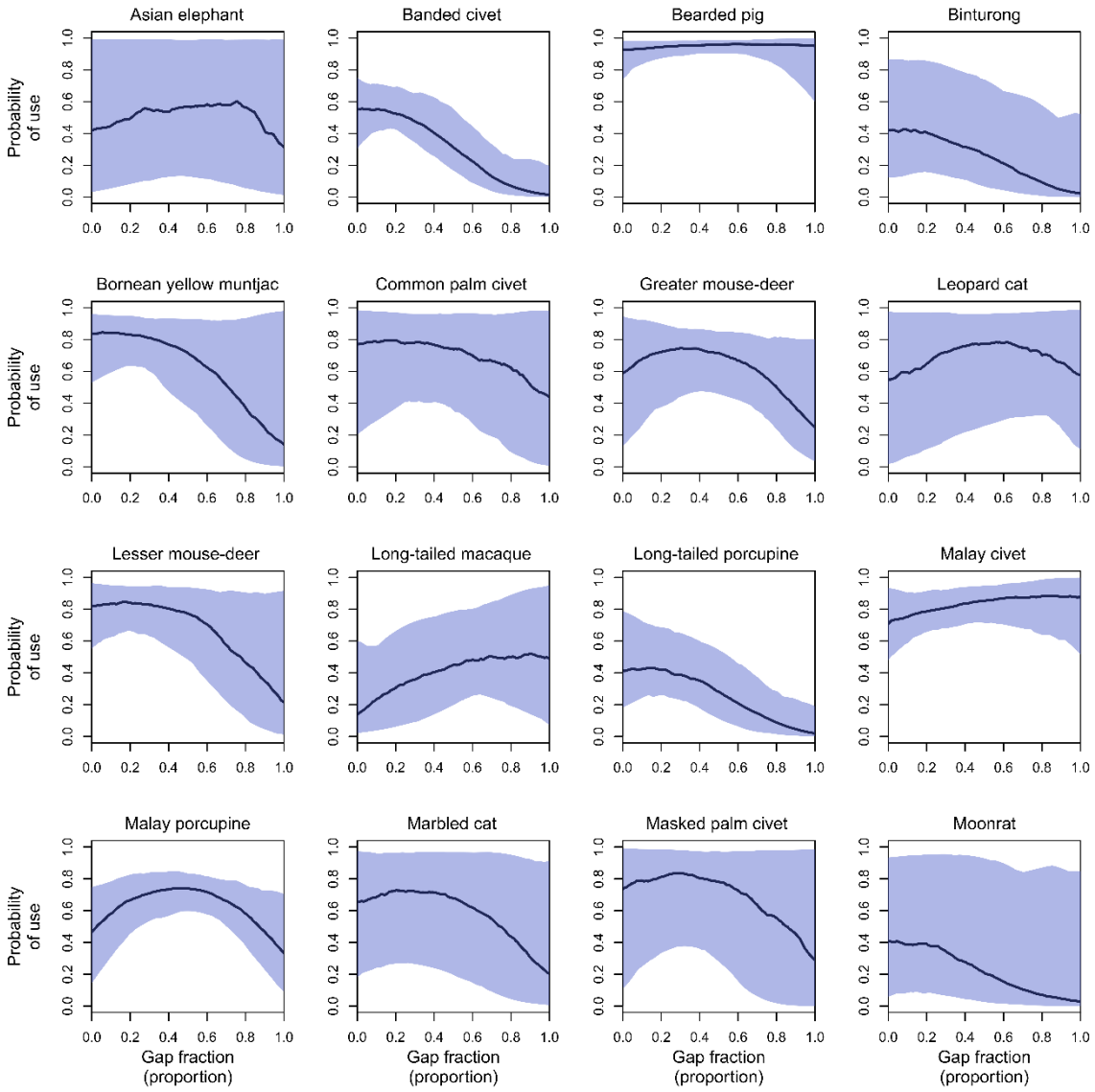
Asian elephant
Banded civet
Bearded pig
Binturong
Bornean yellow muntjac
Common palm civet
Greater mouse-deer
Leopard cat
Lesser mouse-deer
Long-tailed macaque
Long-tailed porcupine
Malay civet
Malay porcupine
Marbled cat
Masked palm civet
Moonrat
Probability of use
Gap fraction (proportion)
0.0
0.2
0.4
0.6
0.8
1.0

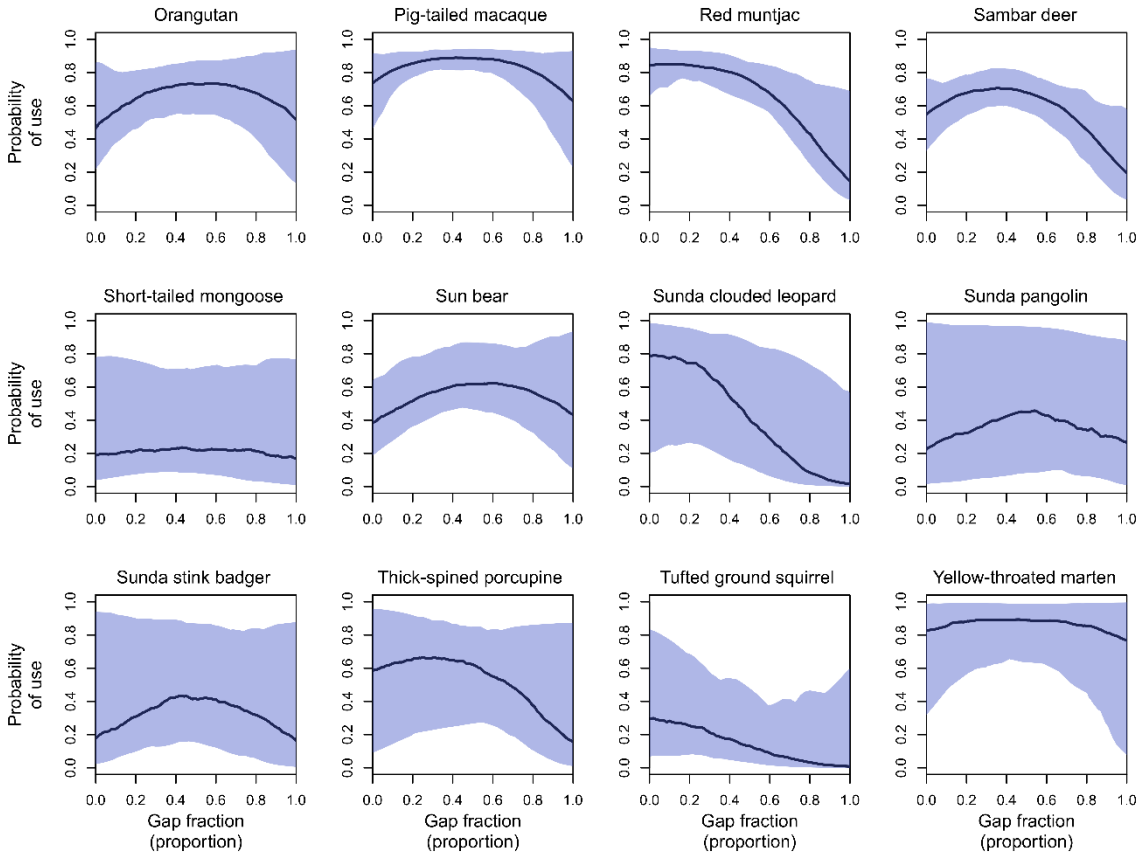

Figure S5: Probability-of-use relative to gap fraction. We quantify gap fraction as the proportion of canopy gaps (< 5 m in height) within a 250 m radius of the camera trap. Outputs are presented for the 28 medium-large terrestrial mammals encountered during sampling. Predicted posterior mean distribution values are presented in dark blue, while uncertainty, as indicated using 95% Bayesian credible intervals is visualized in light blue.

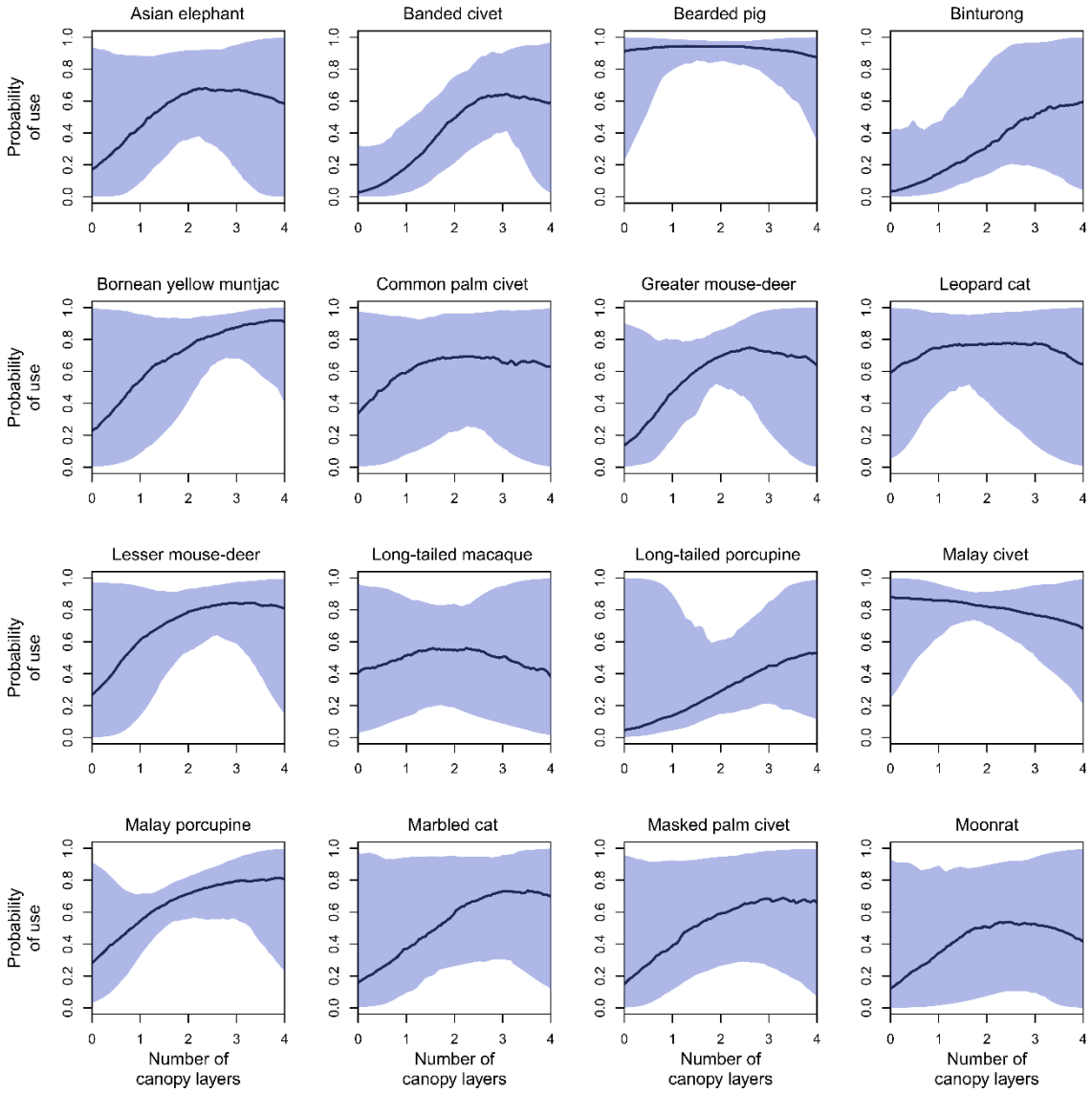
Asian elephant
Banded civet
Bearded pig
Binturong
Bornean yellow muntjac
Common palm civet
Greater mouse-deer
Leopard cat
Lesser mouse-deer
Long-tailed macaque
Long-tailed porcupine
Malay civet
Malay porcupine
Marbled cat
Masked palm civet
Moonrat
Probability of use
Number of canopy layers
0.0 0.2 0.4 0.6 0.8 1.0
0 1 2 3 4

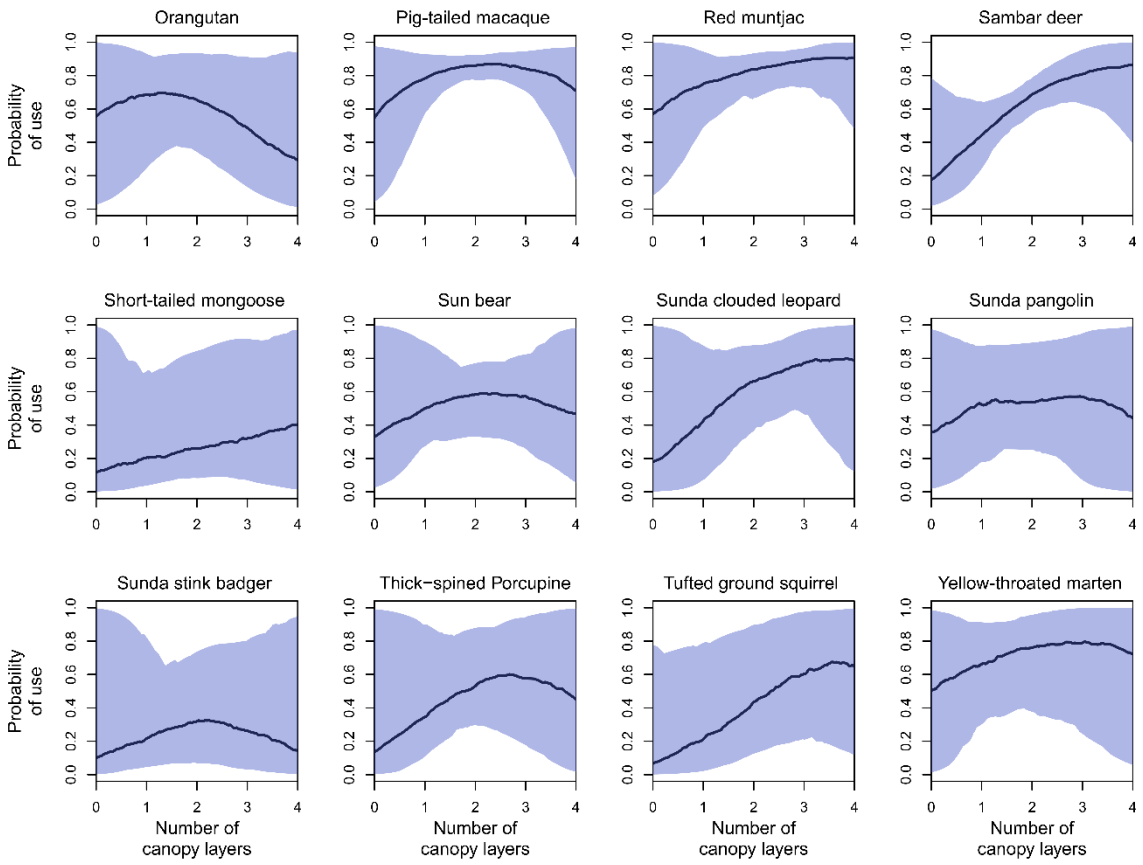

Figure S6: Probability-of-use relative to the number of contiguous layers of vegetation within the canopy. Outputs are presented for the 28 medium-large terrestrial mammals encountered during sampling. Predicted posterior mean distribution values are presented in dark blue, while uncertainty, as indicated using 95% Bayesian credible intervals is visualized in light blue.

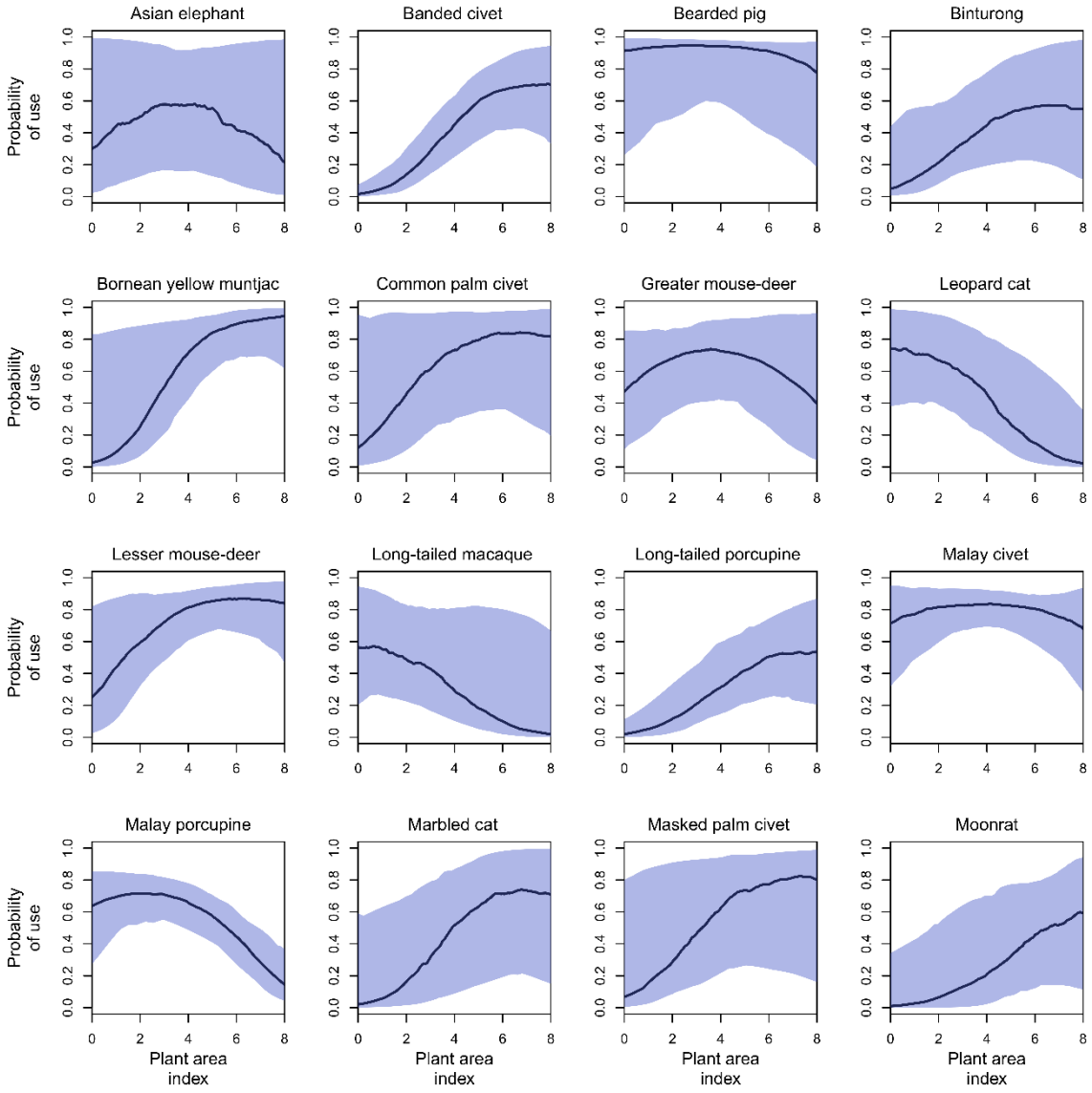
Asian elephant
Banded civet
Bearded pig
Binturong
Bornean yellow muntjac
Common palm civet
Greater mouse-deer
Leopard cat
Lesser mouse-deer
Long-tailed macaque
Long-tailed porcupine
Malay civet
Malay porcupine
Marbled cat
Masked palm civet
Moonrat
Probability of use
Plant area index
0.0 0.2 0.4 0.6 0.8 1.0
0 2 4 6 8

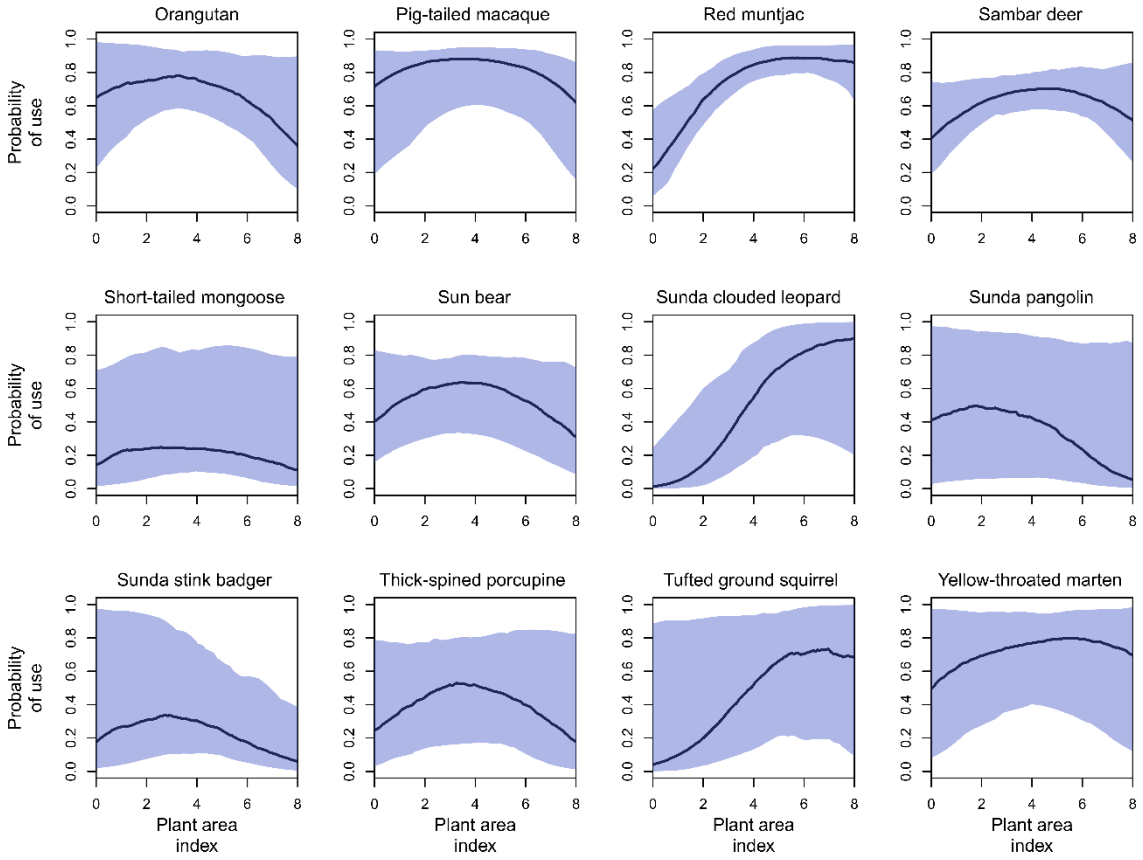

Figure S7: Probability-of-use relative to plant area index. Outputs are presented for the 28 medium-large terrestrial mammals encountered during sampling. Predicted posterior mean distribution values are presented in dark blue, while uncertainty, as indicated using 95% Bayesian credible intervals is visualized in light blue.

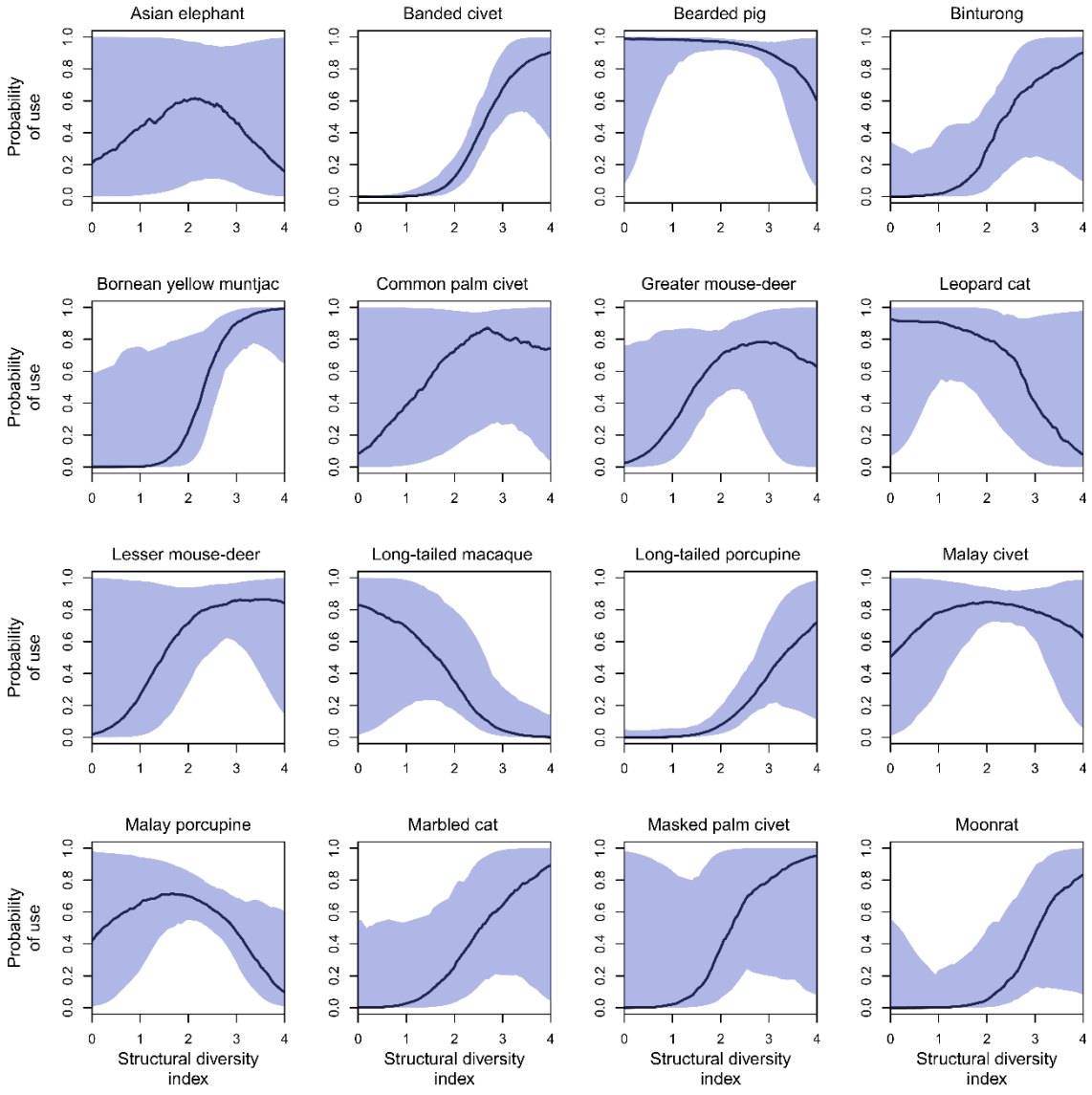
Asian elephant
Banded civet
Bearded pig
Binturong
Bornean yellow muntjac
Common palm civet
Greater mouse-deer
Leopard cat
Lesser mouse-deer
Long-tailed macaque
Long-tailed porcupine
Malay civet
Malay porcupine
Marbled cat
Masked palm civet
Moonrat
Probability of use
Structural diversity index
0.0 0.2 0.4 0.6 0.8 1.0
0 1 2 3 4

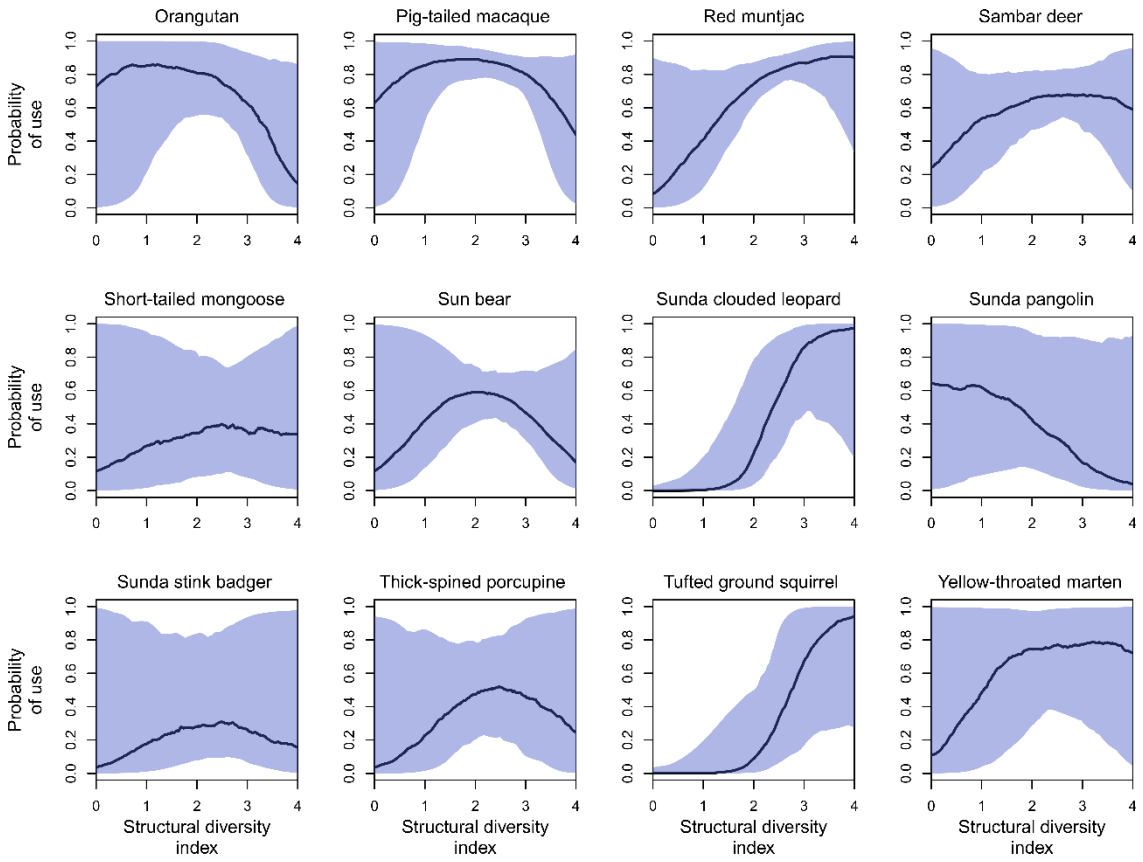

Figure S8: Probability-of-use relative to the structural diversity index. This measure is indicative of niche availability and calculated as the Shannon Index of the plant area distribution. Outputs are presented for the 28 medium-large terrestrial mammals encountered during sampling. Predicted posterior mean distribution values are presented in dark blue, while uncertainty, as indicated using 95% Bayesian credible intervals is visualized in light blue.

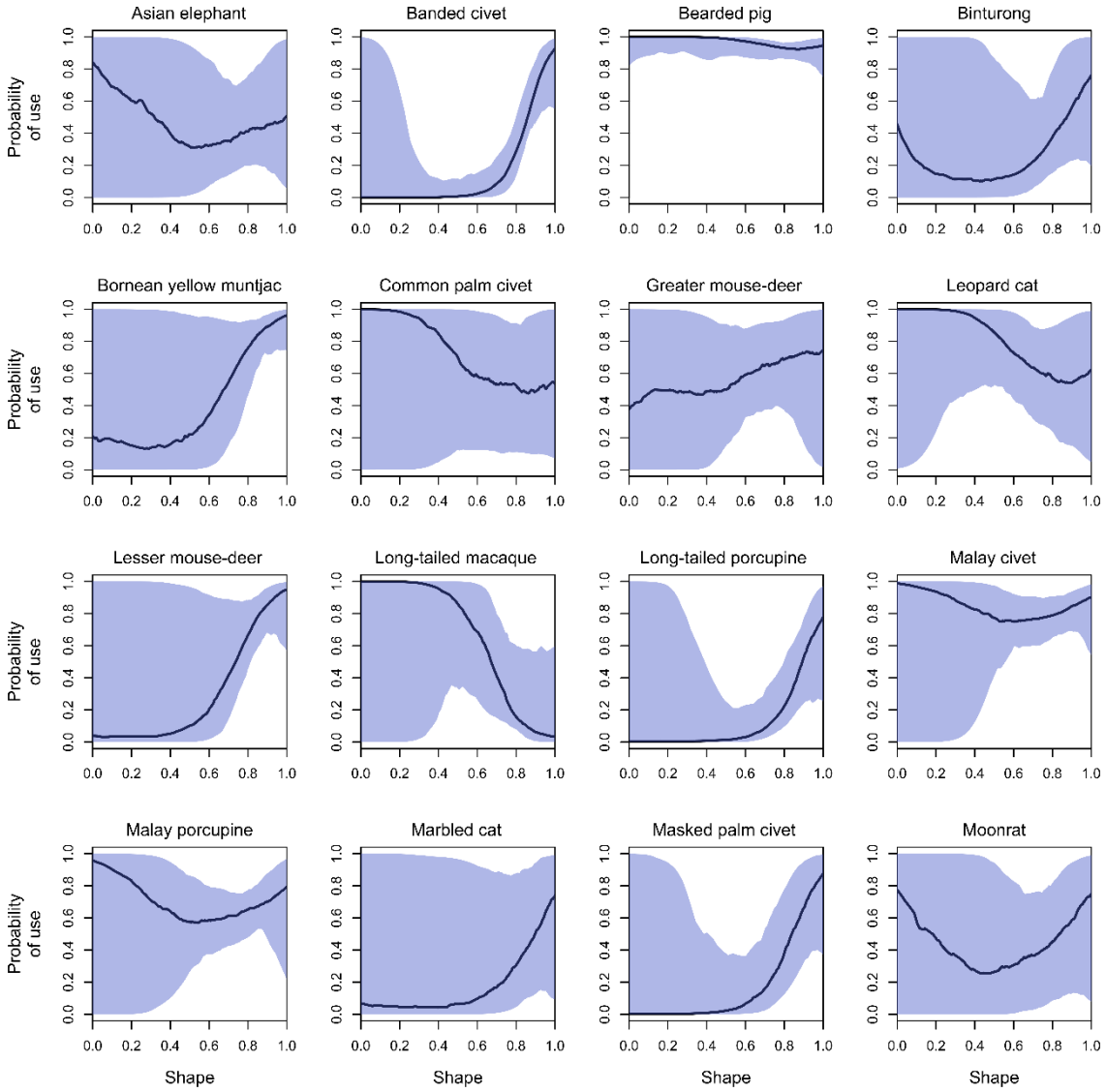
Asian elephant
Banded civet
Bearded pig
Binturong
Bornean yellow muntjac
Common palm civet
Greater mouse-deer
Leopard cat
Lesser mouse-deer
Long-tailed macaque
Long-tailed porcupine
Malay civet
Malay porcupine
Marbled cat
Masked palm civet
Moonrat
Probability of use
Shape
0.0 0.2 0.4 0.6 0.8 1.0

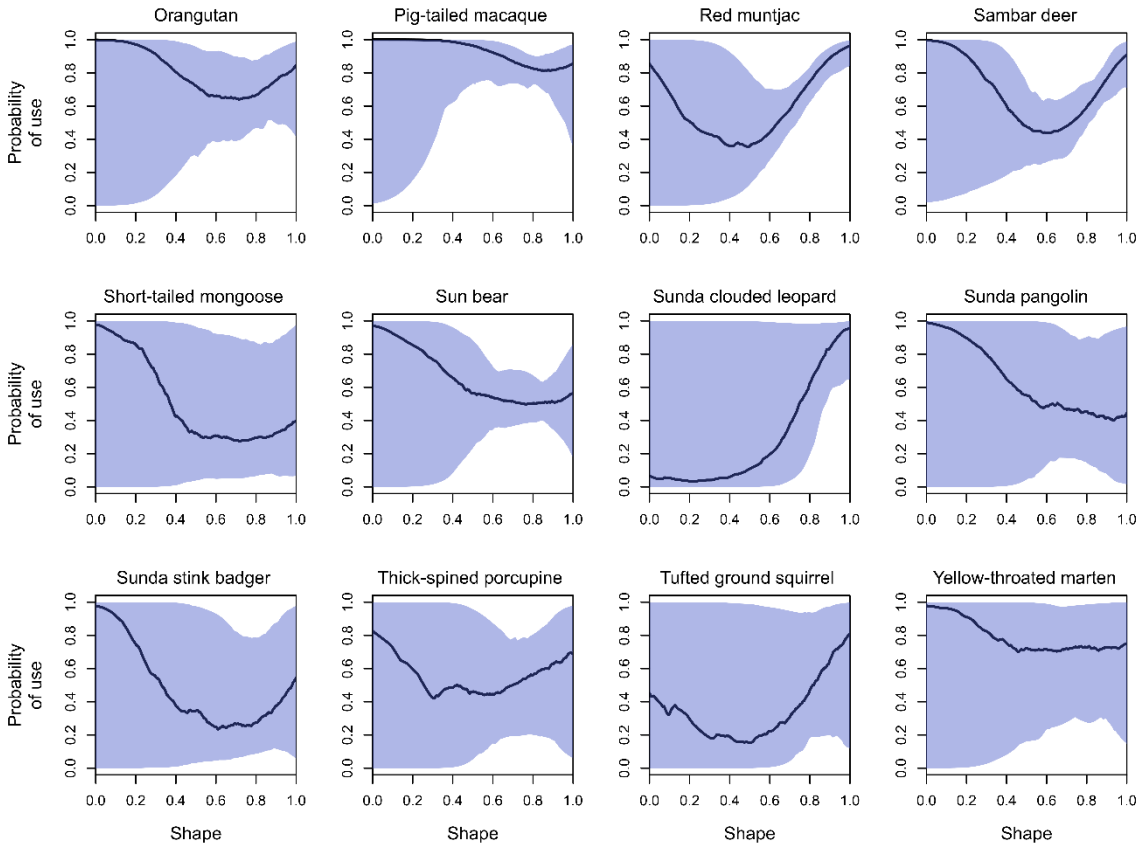

Figure S9: Probability-of-use relative to shape. We define shape as the distribution of vegetation throughout the vertical column. Outputs are presented for the 28 medium-large terrestrial mammals encountered during sampling. Predicted posterior mean distribution values are presented in dark blue, while uncertainty, as indicated using 95% Bayesian credible intervals is visualized in light blue.

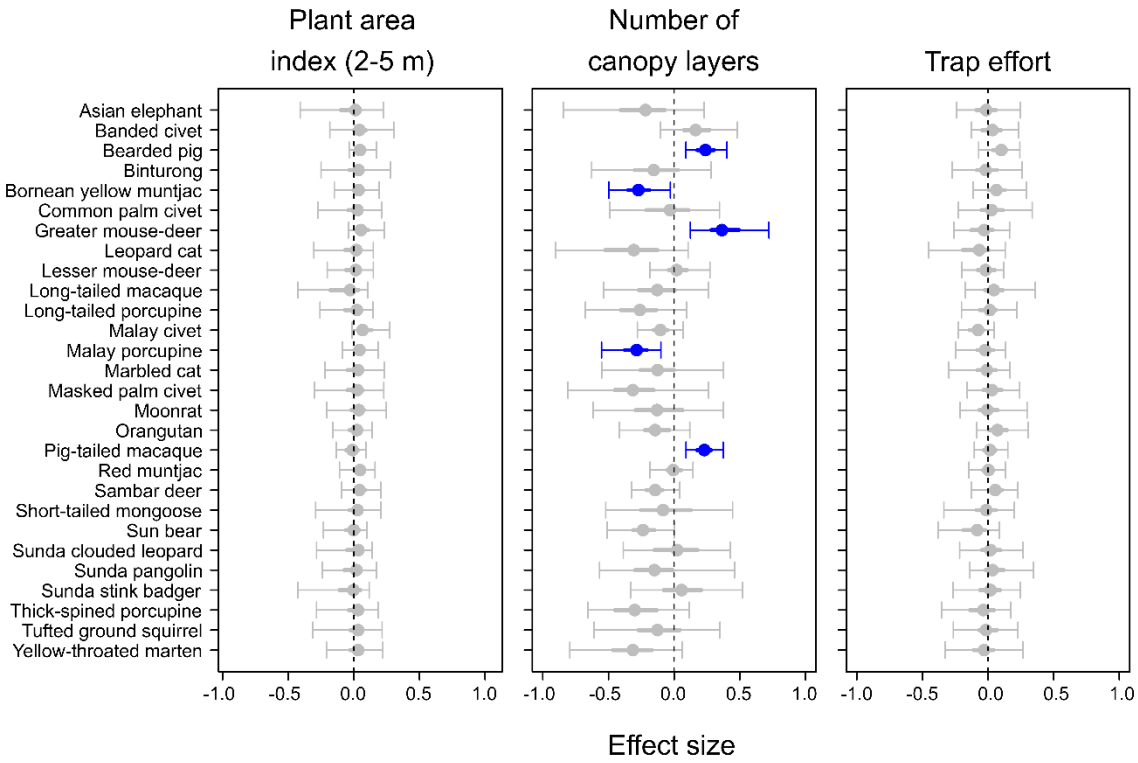

Figure S10: Environmental and sampling covariates influencing detection probability. Outputs are presented for the 28 medium-large terrestrial mammals encountered during sampling. Effect sizes are presented as posterior means (points) and 95% Bayesian credible intervals (BCI). Effects were considered substantial if the 95% BCI did not overlap zero (vertical dashed line). Responsive species are presented in blue.

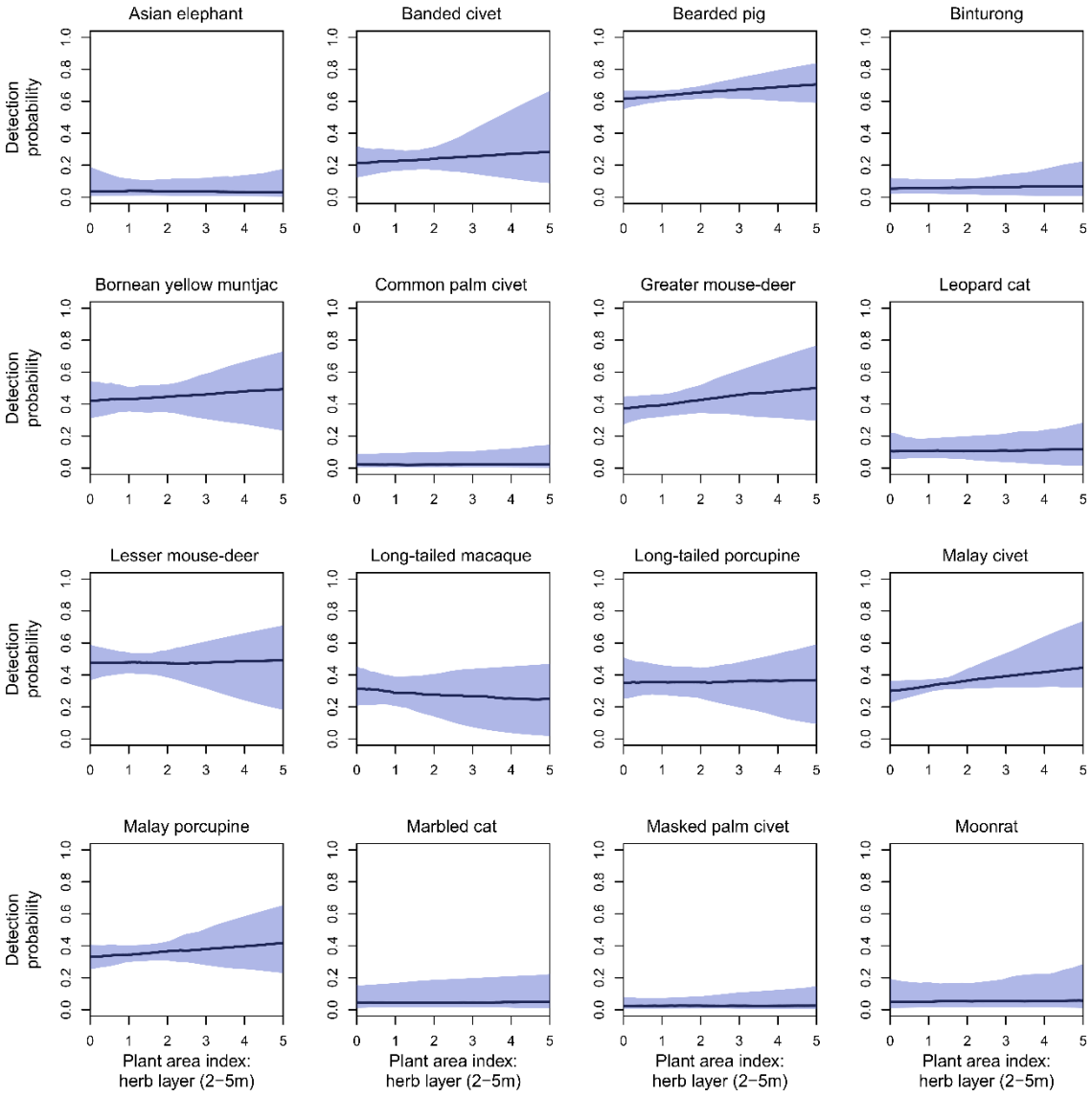
Asian elephant
Banded civet
Bearded pig
Binturong
Bornean yellow muntjac
Common palm civet
Greater mouse-deer
Leopard cat
Lesser mouse-deer
Long-tailed macaque
Long-tailed porcupine
Malay civet
Malay porcupine
Marbled cat
Masked palm civet
Moonrat
Detection probability
Plant area index: herb layer (2–5m)

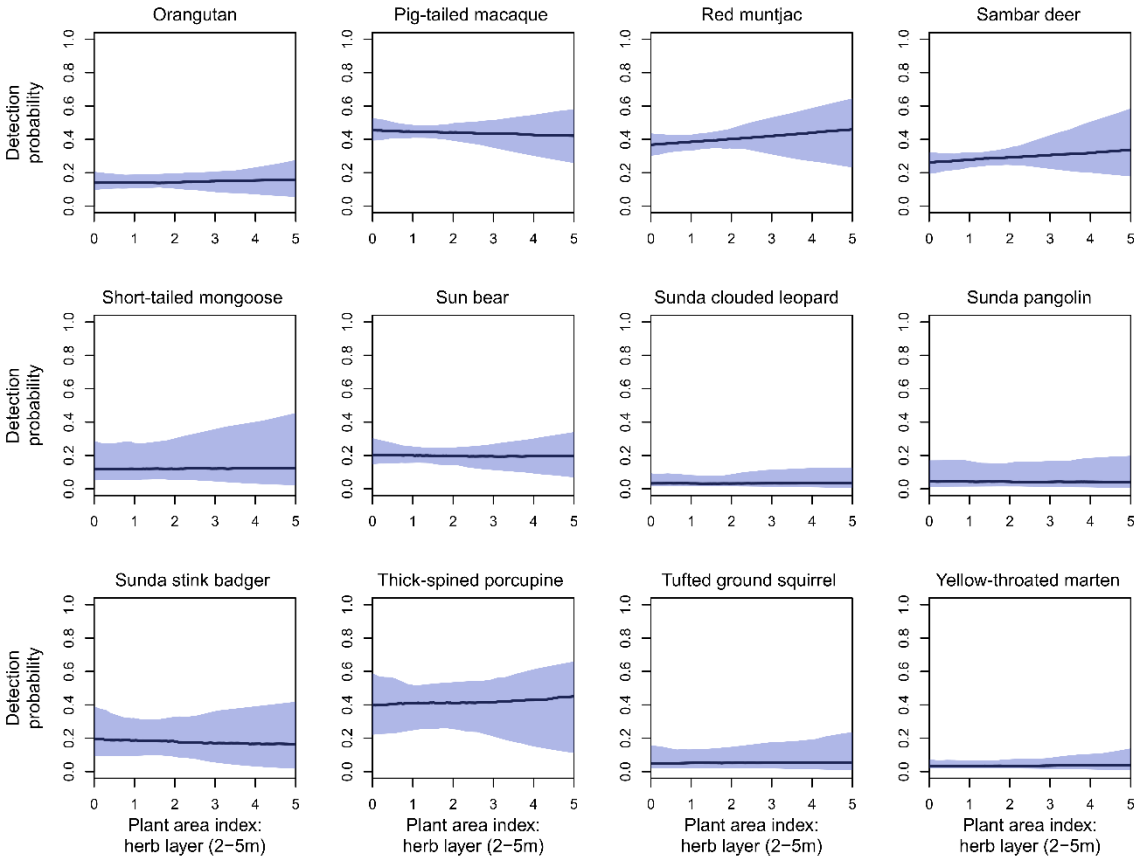

Figure S11: Detection probability relative to plant area index in the herbaceous layer (2-5 m). Outputs are presented for the 28 medium-large terrestrial mammals encountered during sampling. Predicted posterior mean distribution values are presented in dark blue, while uncertainty, as indicated using 95% Bayesian credible intervals is visualized in light blue.

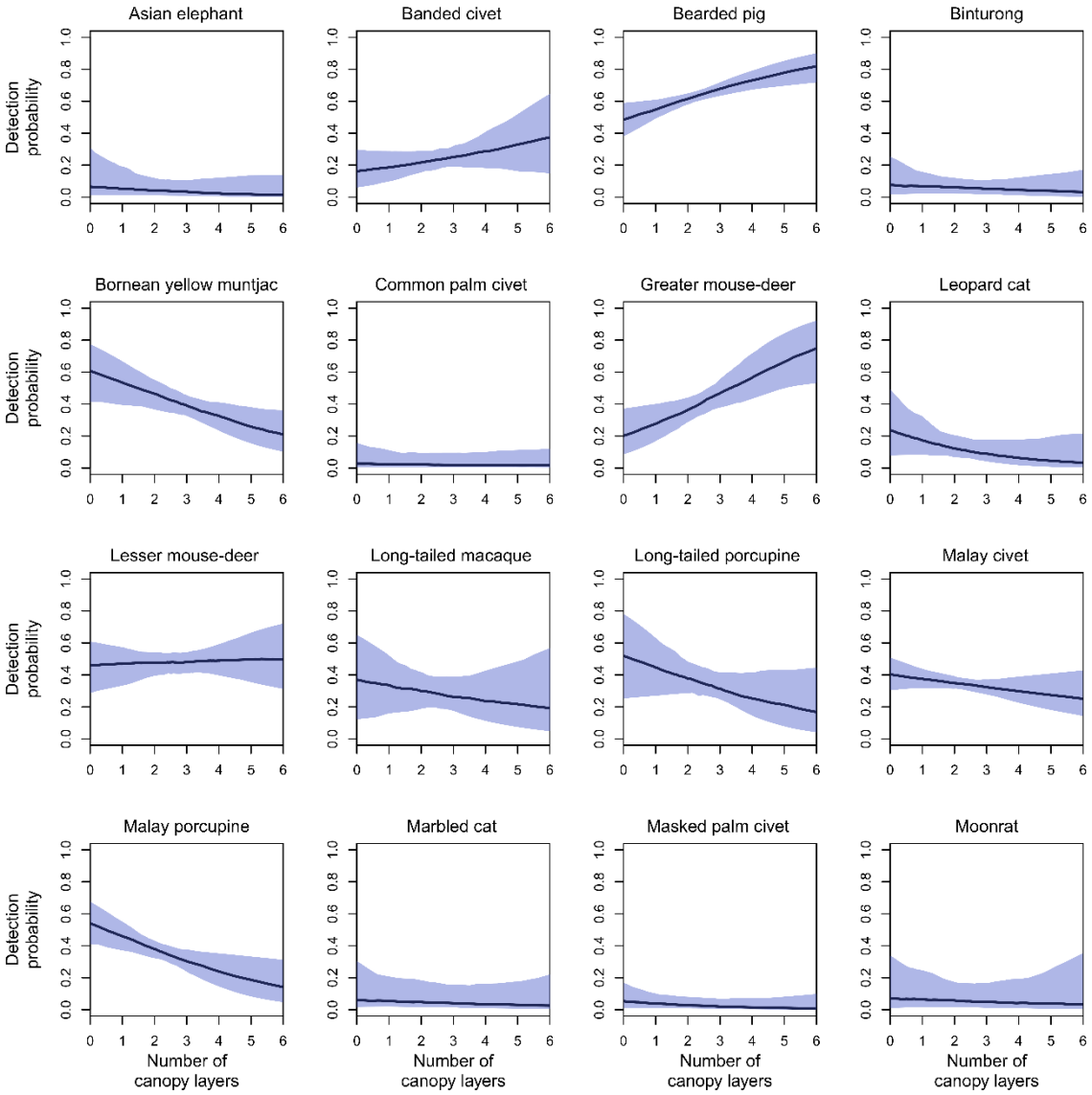
Asian elephant
Banded civet
Bearded pig
Binturong
Bornean yellow muntjac
Common palm civet
Greater mouse-deer
Leopard cat
Lesser mouse-deer
Long-tailed macaque
Long-tailed porcupine
Malay civet
Malay porcupine
Marbled cat
Masked palm civet
Moonrat
Detection probability
Number of canopy layers

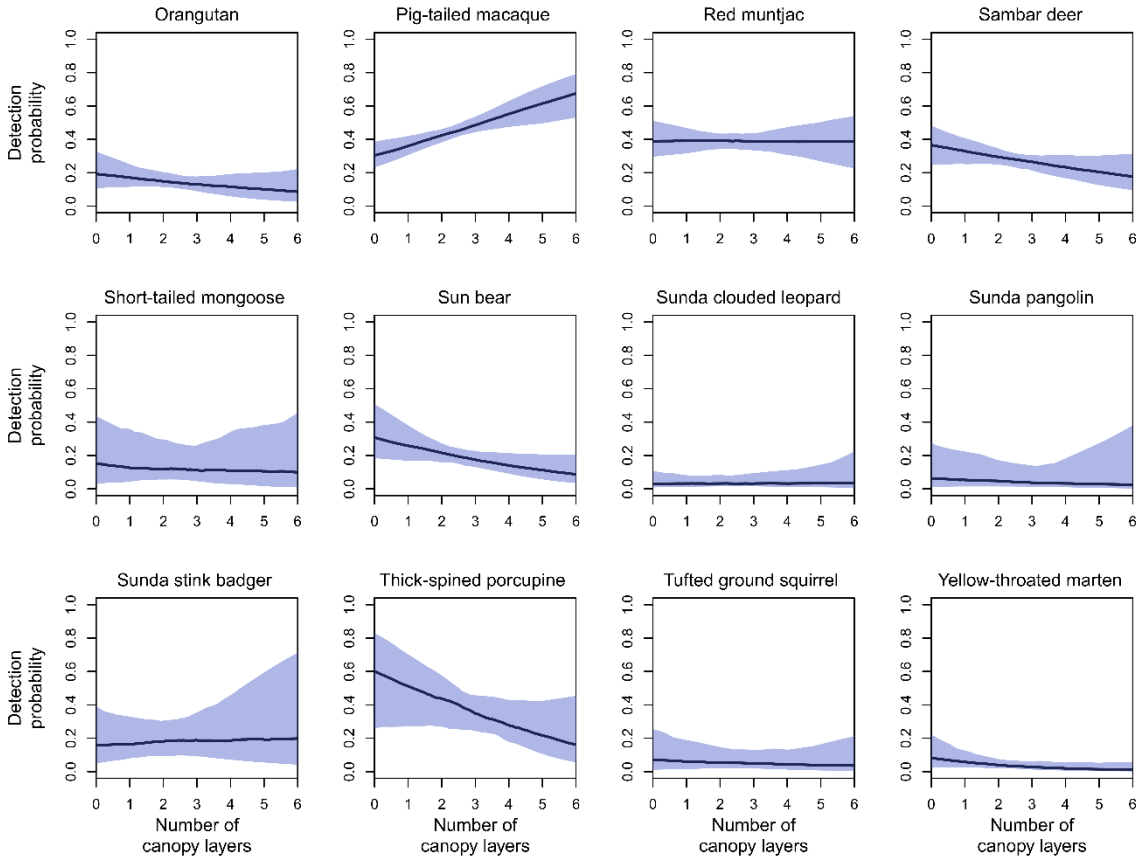

Figure S12: Detection probability relative to the number of contiguous layers of vegetation in the canopy. Outputs are presented for the 28 medium-large terrestrial mammals encountered during sampling. Predicted posterior mean distribution values are presented in dark blue, while uncertainty, as indicated using 95% Bayesian credible intervals is visualized in light blue.

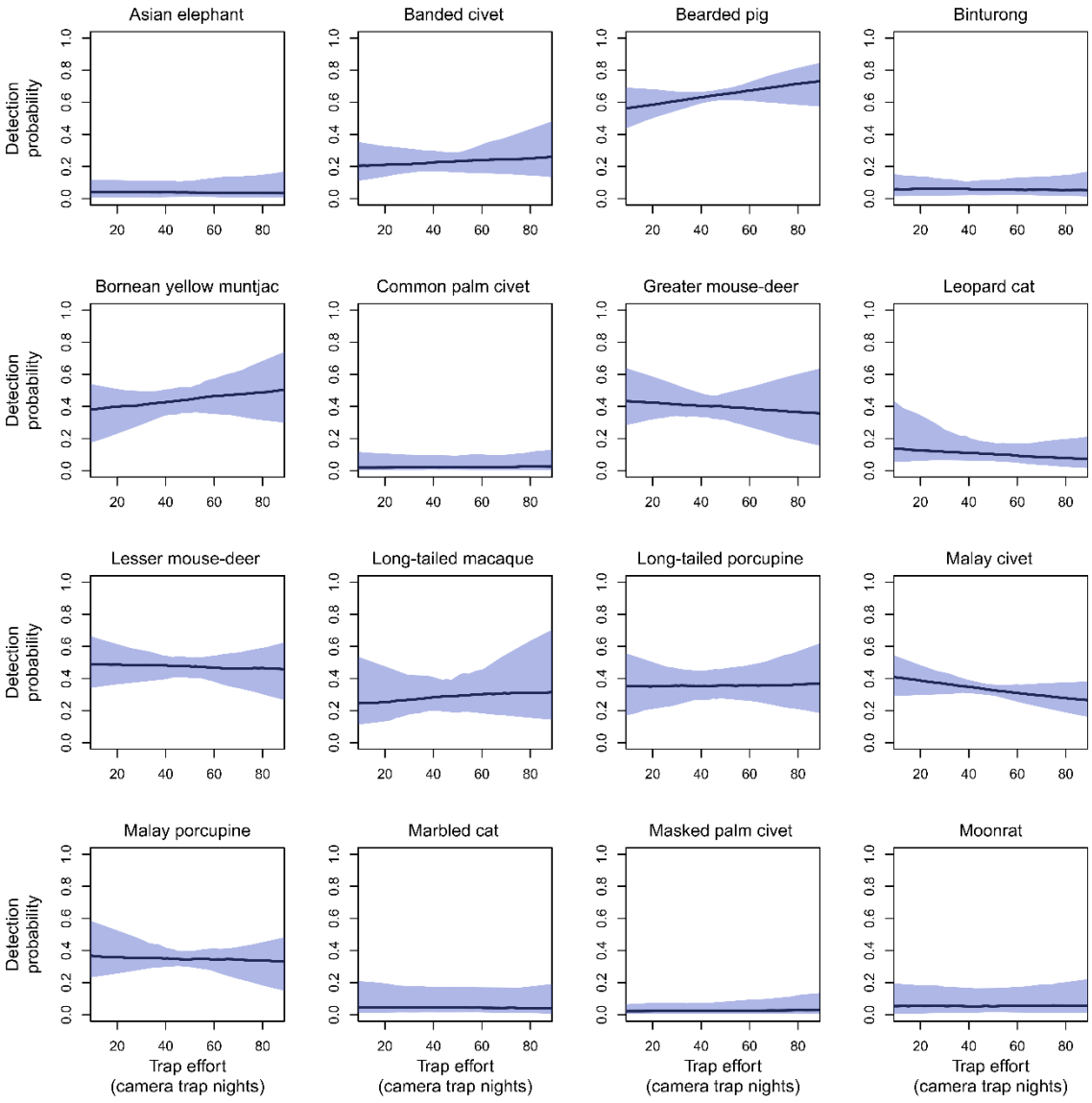
Asian elephant
Banded civet
Bearded pig
Binturong
Bornean yellow muntjac
Common palm civet
Greater mouse-deer
Leopard cat
Lesser mouse-deer
Long-tailed macaque
Long-tailed porcupine
Malay civet
Malay porcupine
Marbled cat
Masked palm civet
Moonrat
Detection probability
0.0 0.2 0.4 0.6 0.8 1.0
20 40 60 80
Trap effort
(camera trap nights)

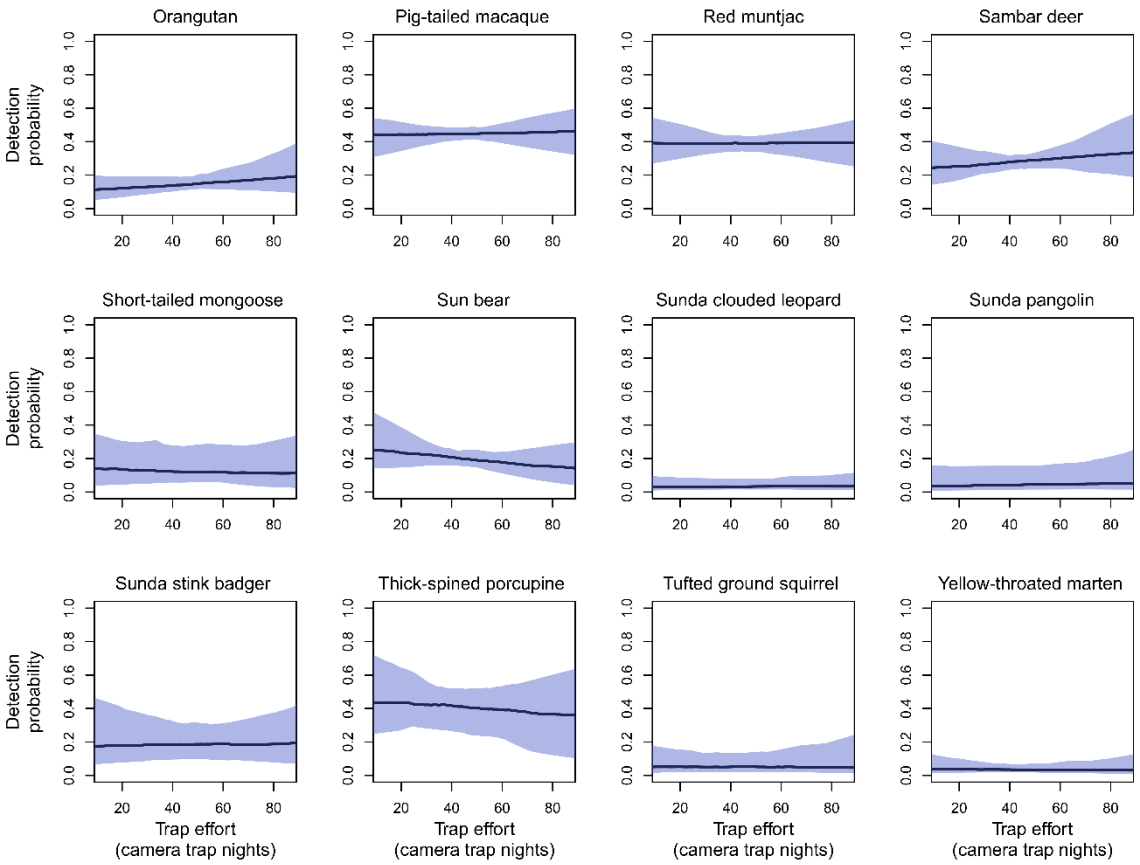

Figure S13: Detection probability relative to sampling effort. We define sampling effort based on the number of nights each camera trap station was operational. Outputs are presented for the 28 medium-large terrestrial mammals encountered during sampling. Predicted posterior mean distribution values are presented in dark blue, while uncertainty, as indicated using 95% Bayesian credible intervals is visualized in light blue.

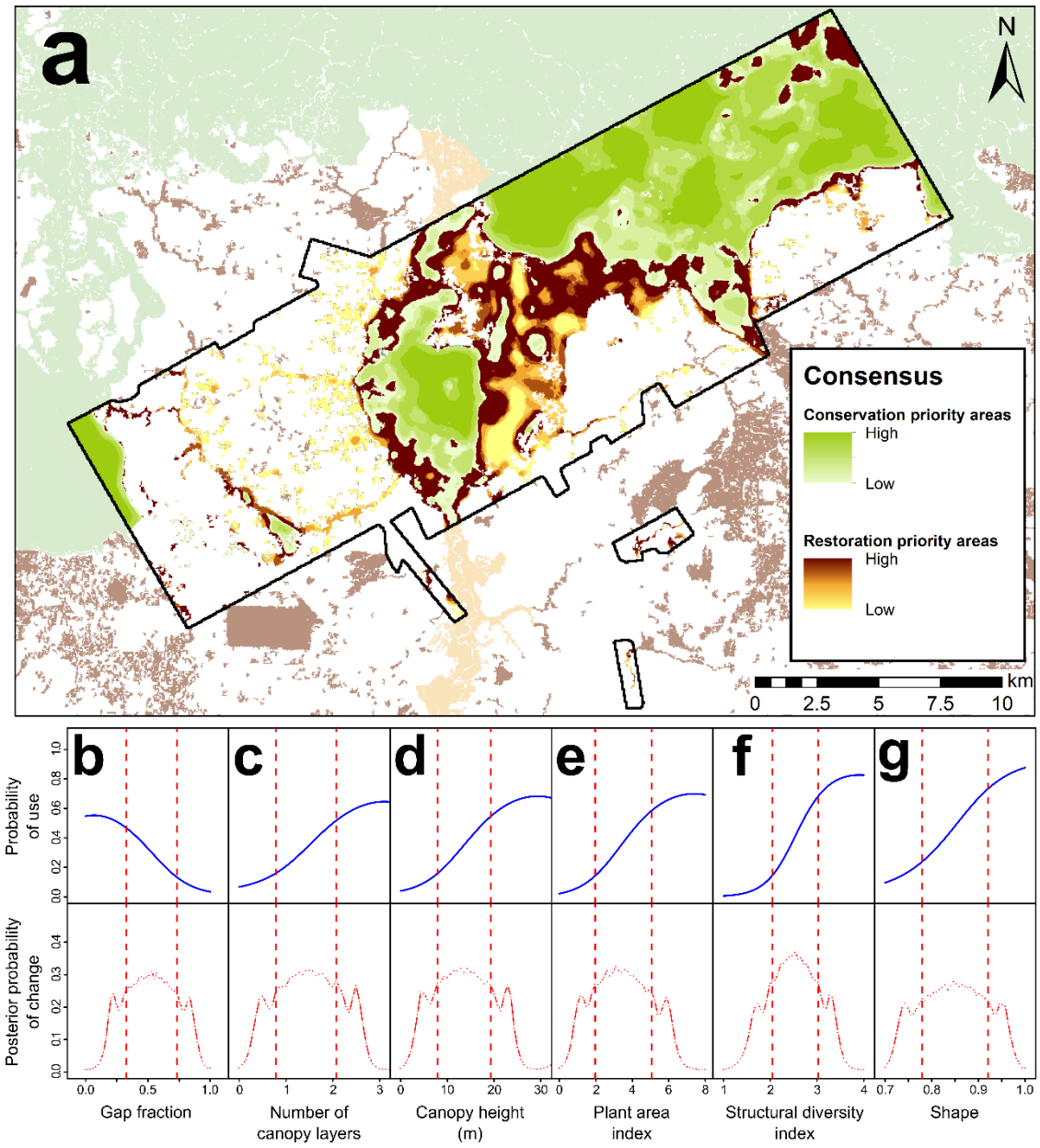

Figure S14: A spatial delineation of conservation and restoration priority areas for the banded civet (*Hemigalus derbyamus*). Priority conservation and restoration areas (a) as predicted by Bayesian change point analysis on predicted occupancy trends (blue lines) relative to informative structural characteristics (b-g). Vertical dashed red lines (b-g)

represent the lower and upper bounds of the zone of transition, characterized in red line graphs by the highest posterior probability of change.

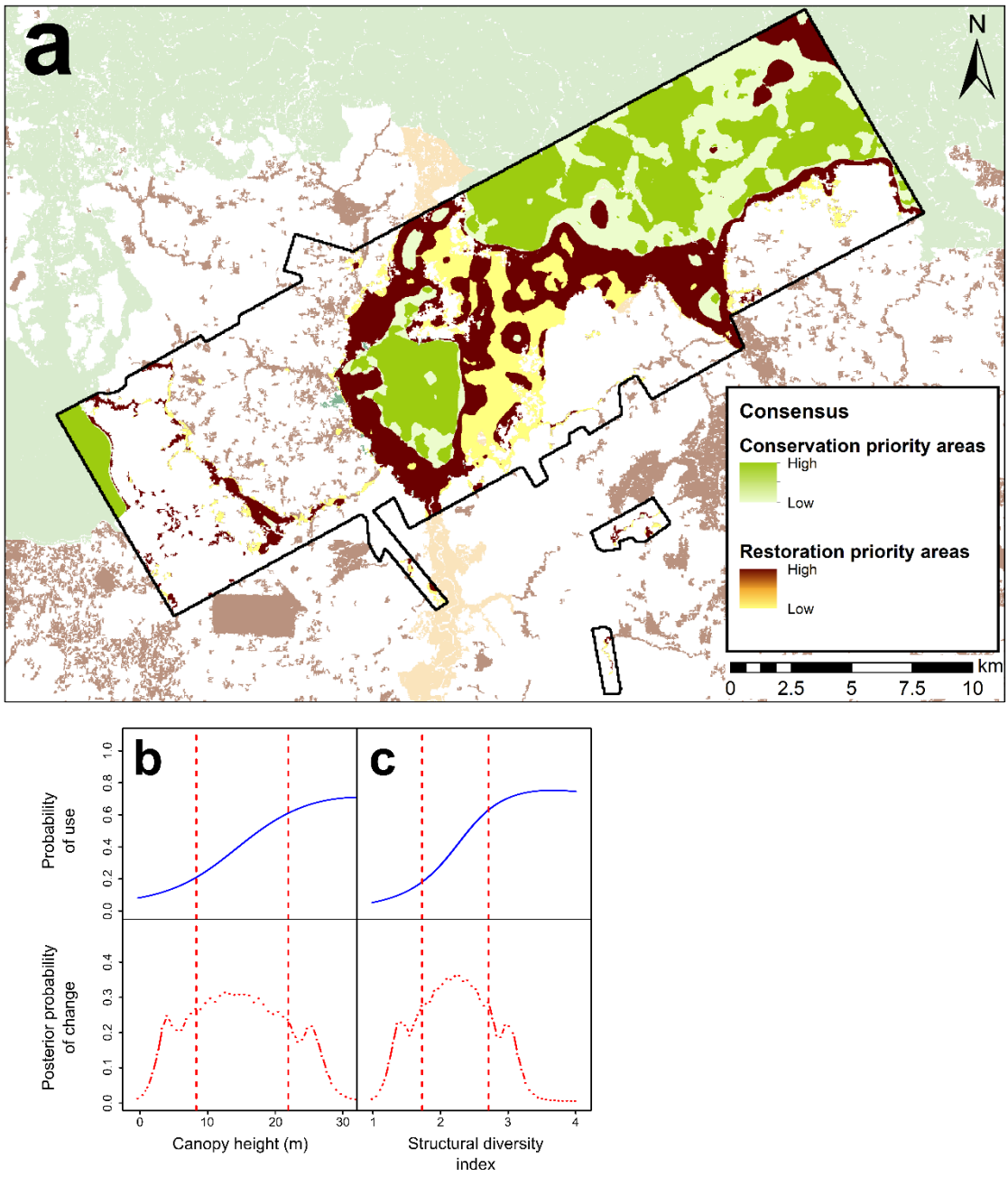

Figure S15: A spatial delineation of conservation and restoration priority areas for the binturong (*Arctictis binturong*). Priority conservation and restoration areas (a) as predicted by Bayesian change point analysis on predicted occupancy trends (blue lines) relative to informative structural characteristics (b-c). Vertical dashed red lines represent the lower

and upper bounds of the zone of transition, characterized in red line graphs by the highest posterior probability of change.

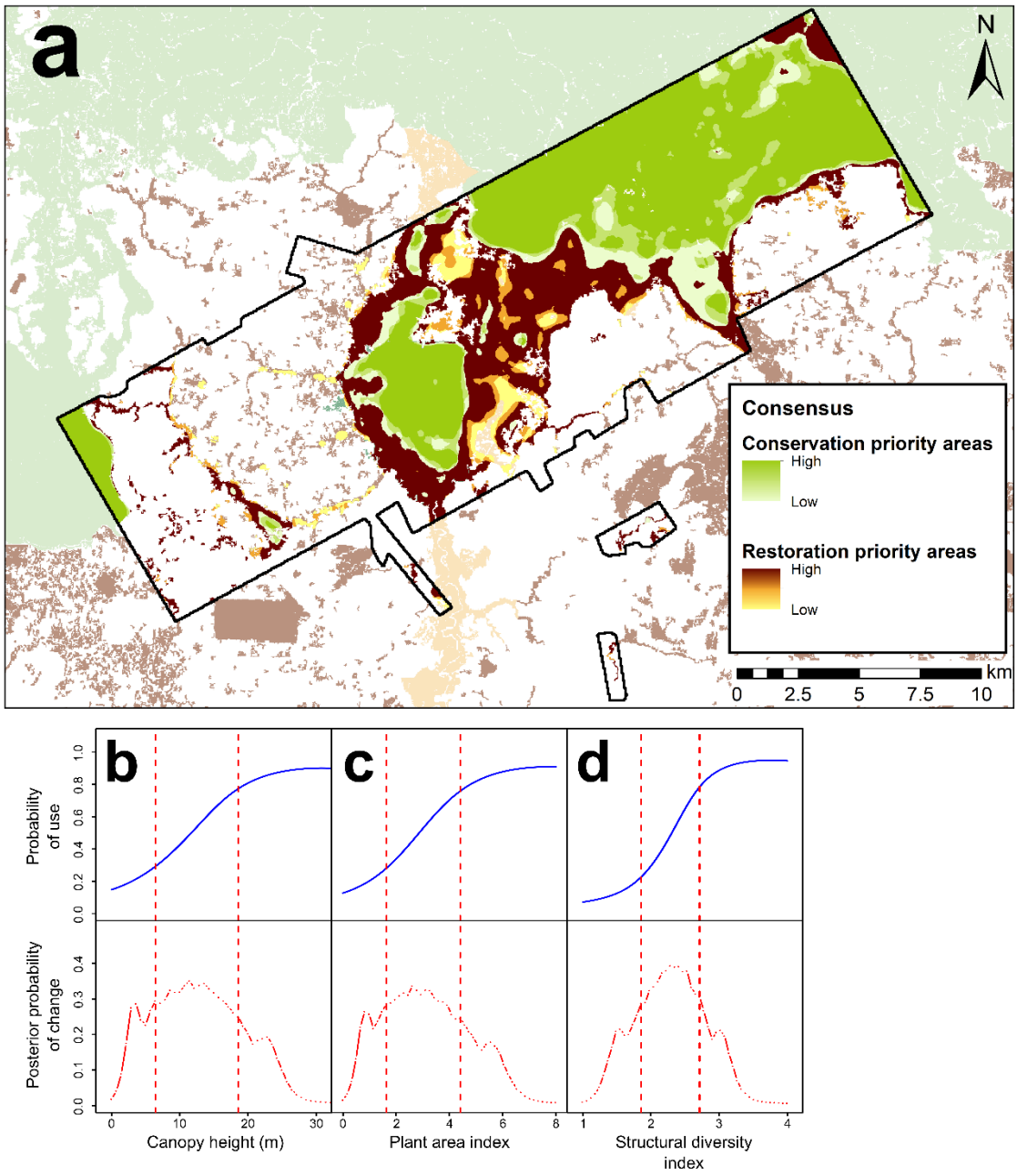

Figure S16: A spatial delineation of conservation and restoration priority areas for the Bornean yellow muntjac (*Muntiacus atherodes*). Priority conservation and restoration areas (a) as predicted by Bayesian change point analysis on predicted occupancy trends (blue lines) relative to informative structural characteristics (b-d). Vertical dashed red lines

represent the lower and upper bounds of the zone of transition, characterized in red line graphs by the highest posterior probability of change.

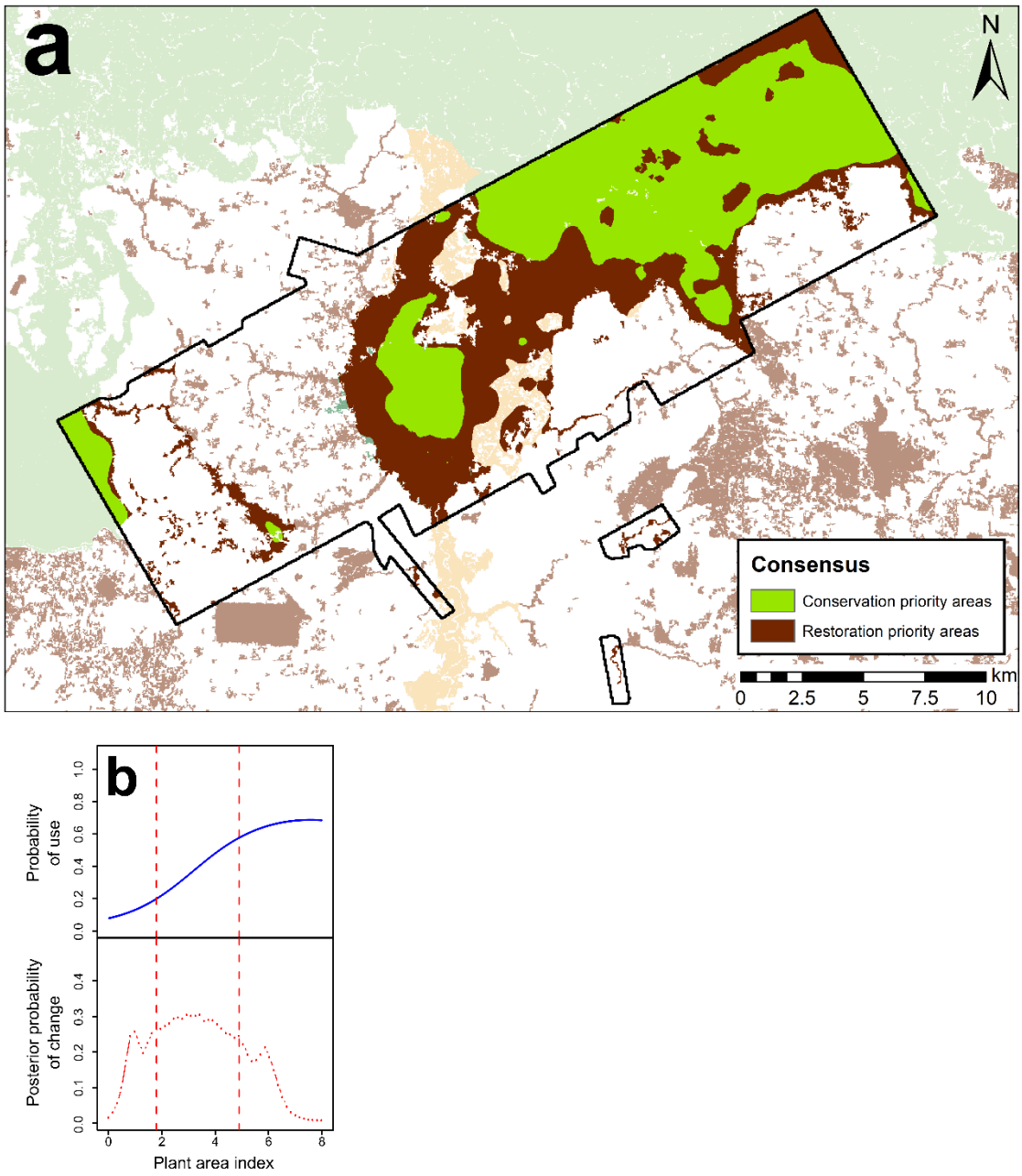

Figure S17: A spatial delineation of conservation and restoration priority areas for the marbled cat (*Pardofelis marmorata*). Priority conservation and restoration areas (a) as predicted by Bayesian change point analysis on predicted occupancy trends (blue lines)

relative to informative structural characteristics (b). The vertical dashed red line represent the lower and upper bounds of the zone of transition, characterized on the red line graph by the highest posterior probability of change.

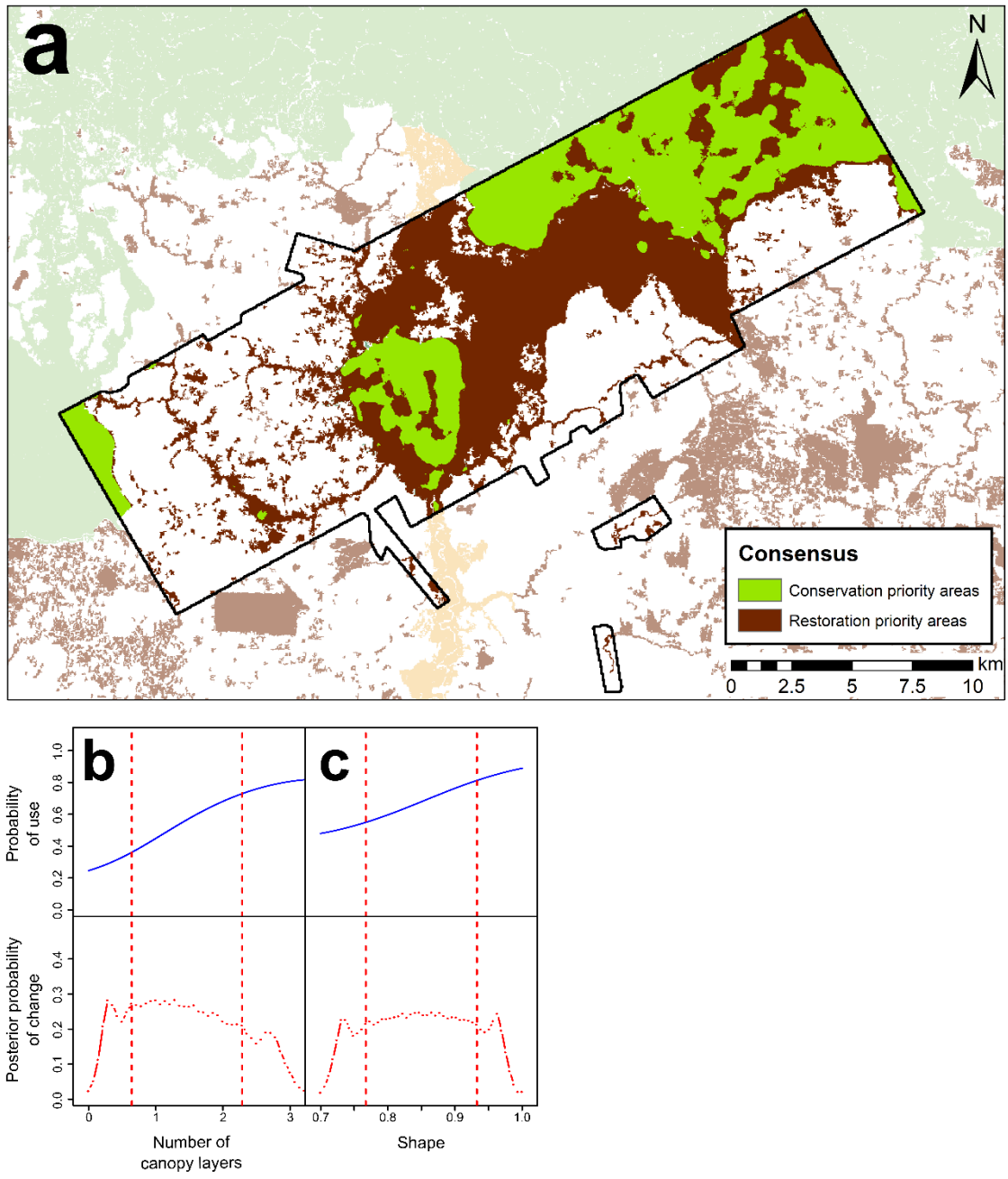

Figure S18: A spatial delineation of conservation and restoration priority areas for the sambar deer (*Rusa unicolor*). Priority conservation and restoration areas (a) as predicted by Bayesian change point analysis on predicted occupancy trends (blue lines) relative to informative structural characteristics (b-c). Vertical dashed red lines represent the lower

and upper bounds of the zone of transition, characterized in red line graphs by the highest posterior probability of change.

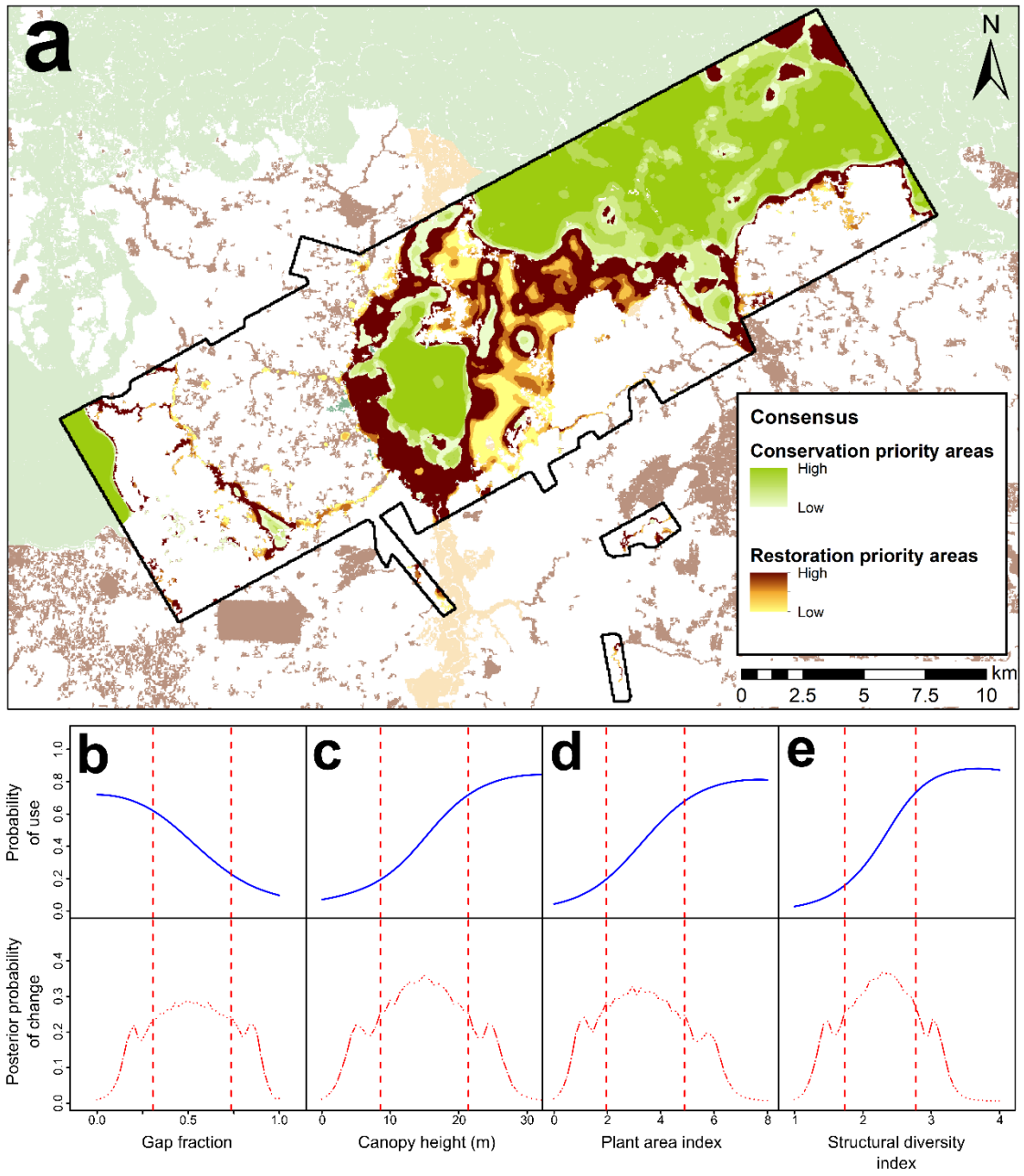

Figure S19: A spatial delineation of conservation and restoration priority areas for the Sunda clouded leopard (*Neofelis diardi*). Priority conservation and restoration areas (a) as predicted by Bayesian change point analysis on predicted occupancy trends (blue lines) relative to informative structural characteristics (b-e). Vertical dashed red lines represent

the lower and upper bounds of the zone of transition, characterized in red line graphs by the highest posterior probability of change.

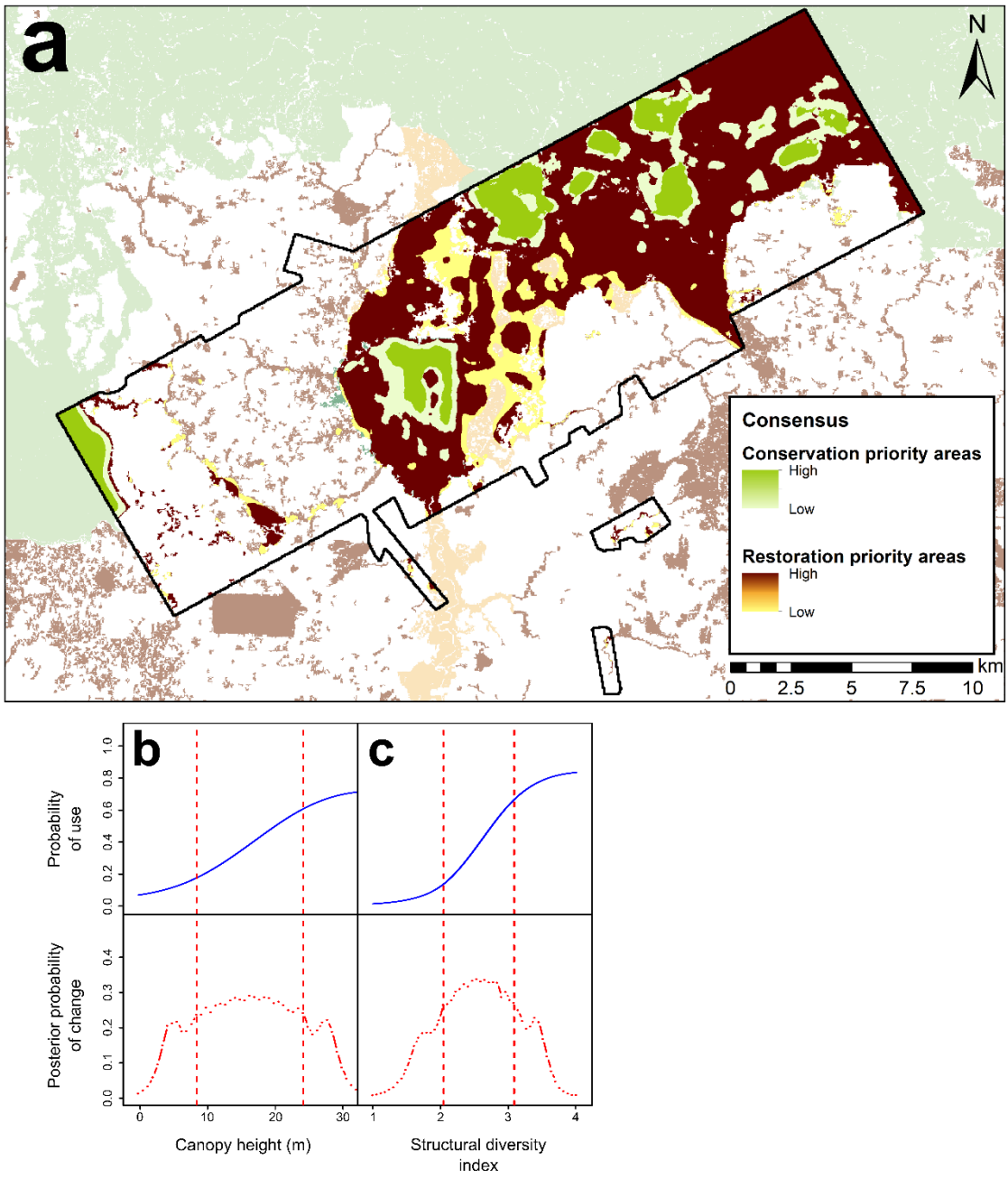

Figure S20: A spatial delineation of conservation and restoration priority areas for the tufted ground squirrel (*Rheithrosciurus macrotis*). Priority conservation and restoration areas (a) as predicted by Bayesian change point analysis on predicted occupancy trends (blue lines) relative to informative structural characteristics (b-c). Vertical dashed red lines

represent the lower and upper bounds of the zone of transition, characterized in red line graphs by the highest posterior probability of change.

Table S1: Response of forest architectural properties to structural degradation. Using outputs from a mean parameterization of a Bayesian linear model, we detail average structural covariate value across each degradation class (Old Growth, Managed Forest, Heavily-degraded Forest, Remnant Forest) and structural differences between classes. Parameter estimates are presented as the mean, standard deviation, 2.5th and 97.5th percentile values of posterior distributions. Differences in structural covariates between degradation classes were considered significant if Bayesian credible intervals (2.5th percentile and 97.5th percentile) did not overlap zero (highlighted in bold).

Structural Variable	Parameter	Mean	SD	2.5th Percentile	97.5th Percentile
Canopy height	Old Growth	24.22	1.27	21.82	26.79
	Managed Forest	23.37	1.24	20.92	25.85
	Heavily-degraded Forest	13.95	0.71	12.56	15.31
	Remnant Forest	9.93	0.90	8.14	11.75
	Old Growth vs. Managed	-0.84	1.75	-4.24	2.61
	Old Growth vs. Heavily-degraded	**-10.27**	**1.44**	**-13.15**	**-7.54**
	Old Growth vs. Remnant	**-14.29**	**1.55**	**-17.32**	**-11.28**
	Managed vs. Heavily-degraded	**-9.43**	**1.44**	**-12.21**	**-6.56**
	Managed vs. Remnant	**-13.44**	**1.52**	**-16.46**	**-10.46**
	Heavily-degraded vs. Remnant	**-4.01**	**1.15**	**-6.26**	**-1.73**
Gap fraction	Old Growth	0.24	0.05	0.15	0.34
	Managed Forest	0.09	0.05	0.00	0.18
	Heavily-degraded Forest	0.39	0.03	0.33	0.44
	Remnant Forest	0.61	0.03	0.54	0.67
	Old Growth vs. Managed	**-0.15**	**0.07**	**-0.28**	**-0.03**
	Old Growth vs. Heavily-degraded	**0.14**	**0.05**	**0.04**	**0.25**
	Old Growth vs. Remnant	**0.36**	**0.06**	**0.25**	**0.47**

	Managed vs. Heavily-degraded	**0.29**	**0.05**	**0.19**	**0.40**
	Managed vs. Remnant	**0.51**	**0.06**	**0.40**	**0.63**
	Heavily-degraded vs. Remnant	**0.22**	**0.04**	**0.13**	**0.31**
Number of layers	Old Growth	2.83	0.08	2.66	2.99
	Managed Forest	2.96	0.08	2.79	3.12
	Heavily-degraded Forest	2.47	0.05	2.38	2.56
	Remnant Forest	2.07	0.06	1.95	2.19
	Old Growth vs. Managed	0.13	0.12	-0.10	0.36
	Old Growth vs. Heavily-degraded	-0.36	0.10	-0.55	-0.16
	Old Growth vs. Remnant	-0.75	0.11	-0.96	-0.55
	Managed vs. Heavily-degraded	-0.49	0.10	-0.67	-0.30
	Managed vs. Remnant	-0.88	0.10	-1.08	-0.68
	Heavily-degraded vs. Remnant	-0.39	0.08	-0.55	-0.24
Plant area index	Old Growth	5.24	0.33	4.61	5.89
	Managed Forest	6.71	0.33	6.07	7.36
	Heavily-degraded Forest	3.96	0.19	3.58	4.33
	Remnant Forest	2.08	0.24	1.60	2.56
	Old Growth vs. Managed	**1.47**	**0.46**	**0.54**	**2.35**
	Old Growth vs. Heavily-degraded	**-1.28**	**0.38**	**-2.04**	**-0.54**
	Old Growth vs. Remnant	**-3.16**	**0.41**	**-3.98**	**-2.38**
	Managed vs. Heavily-degraded	**-2.75**	**0.38**	**-3.50**	**-1.99**
	Managed vs. Remnant	**-4.63**	**0.41**	**-5.43**	**-3.82**
	Heavily-degraded vs. Remnant	**-1.89**	**0.31**	**-2.48**	**-1.27**
Structural diversity index	Old Growth	2.76	0.09	2.57	2.94
	Managed Forest	2.69	0.09	2.50	2.86
	Heavily-degraded Forest	1.63	0.05	1.53	1.73
	Remnant Forest	1.35	0.07	1.22	1.48
	Old Growth vs. Managed	-0.07	0.13	-0.32	0.18
	Old Growth vs. Heavily-degraded	**-1.12**	**0.11**	**-1.34**	**-0.91**

	Old Growth vs. Remnant	**-1.40**	**0.11**	**-1.63**	**-1.18**
	Managed vs. Heavily-degraded	**-1.06**	**0.11**	**-1.26**	**-0.85**
	Managed vs. Remnant	**-1.33**	**0.11**	**-1.55**	**-1.11**
	Heavily-degraded vs. Remnant	**-0.28**	**0.08**	**-0.44**	**-0.11**
Shape	Old Growth	0.21	0.03	0.16	0.27
	Managed Forest	0.20	0.03	0.15	0.25
	Heavily-degraded Forest	0.20	0.02	0.17	0.23
	Remnant Forest	0.22	0.02	0.18	0.25
	Old Growth vs. Managed	-0.01	0.04	-0.09	0.06
	Old Growth vs. Heavily-degraded	-0.01	0.03	-0.08	0.05
	Old Growth vs. Remnant	0.00	0.03	-0.06	0.07
	Managed vs. Heavily-degraded	0.00	0.03	-0.06	0.06
	Managed vs. Remnant	0.01	0.03	-0.05	0.08
	Heavily-degraded vs. Remnant	0.02	0.03	-0.03	0.07

Table S2: Model selection, scale optimization and model fit summary statistics. Model selection and scale optimization were based on comparison of Watanabe AIC values, with the lowest scoring WAIC values indicating the overall best model (presented in bold and italics) and the most responsive scales for each structural covariate (presented in bold). We quantify support for competing models using ΔWAIC and WAIC*w*. ΔWAIC indicates variation in WAIC relative to the highest ranked model, we consider equivalent statistical support for models within two ΔWAIC. WAIC*w* describes Akaike weights and specifies the probability that a model is the top ranking formulation amongst the competing candidate set. Model fit was judged using Bayesian *P* values (BPV) and the "lack-of-fit" statistic (Chat). BPV values between 0.05 and 0.95 and Chat scores ~1 indicate adequate model fit. For comparative purposes, we provide model selection and fit statistics for null models (denoted with NA values in the Course- and Fine-scale (m) columns).

Model	Coarse-scale (m)	Fine-scale (m)	BPV	Chat	WAIC	ΔWAIC	WAIC*w*
Forest cover + Forest quality + Canopy height	**2000**	**250**	**0.41**	**1.03**	**2039.60**	**0.00**	**0.66**
	2000	500	0.49	1.02	2041.85	2.25	0.22
	2000	10	0.43	1.03	2043.00	3.40	0.12
	2000	50	0.35	1.03	2073.89	34.29	0.00
	2000	150	0.43	1.02	2074.70	35.10	0.00
	2000	25	0.36	1.03	2082.02	42.42	0.00
	1500	500	0.46	1.02	2089.22	49.62	0.00
	1500	250	0.43	1.02	2095.71	56.11	0.00
	1500	100	0.43	1.01	2100.56	60.96	0.00
	2000	100	0.40	1.02	2109.40	69.80	0.00
	1000	25	0.43	1.02	2112.06	72.46	0.00
	1000	500	0.57	1.00	2112.66	73.06	0.00
	1500	10	0.43	1.02	2113.98	74.38	0.00
	1000	150	0.45	1.01	2115.11	75.51	0.00
	1000	250	0.52	1.00	2144.21	104.61	0.00
	1000	10	0.45	1.01	2150.68	111.08	0.00
	1000	100	0.49	1.02	2152.13	112.53	0.00
	1500	150	0.51	1.01	2166.22	126.62	0.00
	1500	25	0.46	1.01	2169.51	129.91	0.00

	1000	50	0.39	1.02	2177.02	137.42	0.00
	1500	50	0.43	1.02	2217.24	177.64	0.00
	NA	NA	0.39	1.03	2219.60	180.00	0.00
Forest cover + Forest quality +	**2000**	**250**	**0.47**	**1.02**	**2057.30**	**0.00**	**0.56**
Gap fraction	**1000**	**500**	**0.50**	**1.01**	**2059.08**	**1.78**	**0.23**
	2000	500	0.33	1.03	2060.42	3.12	0.12
	2000	150	0.35	1.04	2061.01	3.71	0.09
	1500	10	0.44	1.02	2067.09	9.79	0.00
	1500	500	0.44	1.02	2071.38	14.08	0.00
	1500	150	0.49	1.01	2071.86	14.56	0.00
	2000	10	0.47	1.02	2075.88	18.58	0.00
	1000	50	0.44	1.02	2085.62	28.32	0.00
	1000	150	0.38	1.02	2108.36	51.06	0.00
	1500	50	0.49	1.01	2108.49	51.19	0.00
	2000	50	0.45	1.02	2111.67	54.37	0.00
	1000	100	0.43	1.02	2118.44	61.14	0.00
	2000	25	0.47	1.01	2133.52	76.22	0.00
	1500	100	0.34	1.03	2136.28	78.98	0.00
	1500	250	0.41	1.03	2138.21	80.91	0.00
	1000	10	0.41	1.03	2140.72	83.42	0.00
	2000	100	0.38	1.02	2142.91	85.61	0.00
	1000	25	0.41	1.02	2143.88	86.58	0.00
	1000	250	0.50	1.01	2151.82	94.52	0.00
	1500	25	0.38	1.03	2179.06	121.76	0.00
	NA	NA	0.39	1.03	2219.60	162.30	0.00
Forest cover + Forest quality +	**2000**	**250**	**0.41**	**1.02**	**2072.13**	**0.00**	**1.00**
Number of layers	1500	250	0.41	1.03	2088.62	16.49	0.00
	2000	500	0.38	1.02	2096.35	24.22	0.00
	1000	500	0.51	1.01	2098.42	26.29	0.00
	1500	150	0.43	1.03	2111.04	38.91	0.00
	1500	500	0.40	1.03	2111.11	38.98	0.00
	2000	150	0.43	1.03	2112.24	40.11	0.00
	1500	50	0.40	1.03	2115.06	42.93	0.00
	2000	100	0.44	1.01	2121.95	49.82	0.00
	2000	10	0.47	1.02	2126.80	54.67	0.00
	1500	25	0.43	1.02	2134.85	62.72	0.00
	1500	100	0.40	1.03	2143.96	71.83	0.00
	1000	50	0.39	1.03	2144.92	72.79	0.00
	1000	100	0.41	1.02	2152.17	80.04	0.00
	1000	10	0.44	1.01	2161.04	88.91	0.00
	2000	25	0.38	1.03	2162.80	90.67	0.00
	2000	50	0.49	1.01	2167.38	95.25	0.00
	1000	150	0.37	1.03	2178.11	105.98	0.00
	1000	250	0.46	1.01	2197.16	125.03	0.00
	1500	10	0.40	1.03	2203.62	131.49	0.00
	NA	NA	0.39	1.03	2219.60	147.47	0.00
	1000	25	0.41	1.02	2220.23	148.10	0.00
Forest cover + Forest quality +	***2000***	***500***	***0.46***	***1.01***	***1979.98***	***0.00***	***1.00***
Plant area index	2000	25	0.45	1.02	1996.37	16.39	0.00
	1500	100	0.41	1.02	2027.27	47.29	0.00
	2000	50	0.38	1.02	2049.63	69.65	0.00
	2000	250	0.39	1.02	2061.02	81.04	0.00
	2000	10	0.50	1.01	2076.72	96.74	0.00
	2000	150	0.43	1.02	2079.39	99.41	0.00

	1500	10	0.46	1.01	2085.83	105.85	0.00
	2000	100	0.37	1.04	2089.81	109.83	0.00
	1000	25	0.49	1.01	2094.70	114.72	0.00
	1000	500	0.45	1.01	2101.87	121.89	0.00
	1500	25	0.45	1.02	2107.45	127.47	0.00
	1000	10	0.35	1.03	2110.17	130.19	0.00
	1000	50	0.39	1.02	2113.79	133.81	0.00
	1000	250	0.45	1.01	2117.06	137.08	0.00
	1000	100	0.37	1.03	2122.11	142.13	0.00
	1500	250	0.48	1.01	2125.74	145.76	0.00
	1500	50	0.56	1.01	2128.49	148.51	0.00
	1000	150	0.51	1.01	2133.49	153.51	0.00
	1500	150	0.45	1.02	2147.01	167.03	0.00
	1500	500	0.44	1.01	2156.04	176.06	0.00
	NA	NA	0.39	1.03	2219.60	239.62	0.00
Forest cover + Forest quality + Structural diversity index	**2000**	**500**	**0.45**	**1.02**	**2016.74**	**0.00**	**0.99**
	2000	25	0.49	1.01	2027.01	10.27	0.01
	2000	50	0.41	1.02	2032.58	15.84	0.00
	1500	10	0.37	1.02	2044.55	27.81	0.00
	2000	150	0.45	1.01	2054.50	37.76	0.00
	2000	250	0.48	1.02	2070.89	54.15	0.00
	1500	500	0.40	1.02	2071.30	54.56	0.00
	2000	10	0.39	1.03	2074.32	57.58	0.00
	1000	25	0.49	1.01	2077.82	61.08	0.00
	1000	50	0.49	1.01	2083.64	66.90	0.00
	1500	50	0.52	1.01	2090.21	73.47	0.00
	1000	150	0.41	1.03	2112.02	95.28	0.00
	1000	250	0.39	1.03	2117.09	100.35	0.00
	1500	25	0.37	1.04	2119.33	102.59	0.00
	2000	100	0.46	1.02	2123.47	106.73	0.00
	1500	250	0.41	1.02	2123.93	107.19	0.00
	1000	100	0.45	1.02	2129.03	112.29	0.00
	1000	10	0.44	1.01	2132.22	115.48	0.00
	1500	150	0.41	1.01	2135.54	118.80	0.00
	1500	100	0.45	1.02	2143.25	126.51	0.00
	1000	500	0.40	1.03	2159.95	143.21	0.00
	NA	NA	0.39	1.03	2219.60	202.86	0.00
Forest cover + Forest quality + Shape	**2000**	**500**	**0.40**	**1.03**	**2020.87**	**0.00**	**1.00**
	2000	250	0.44	1.02	2044.24	23.37	0.00
	2000	50	0.42	1.02	2046.02	25.15	0.00
	2000	100	0.45	1.02	2047.44	26.57	0.00
	1500	25	0.37	1.03	2054.64	33.77	0.00
	2000	10	0.43	1.02	2062.02	41.15	0.00
	2000	150	0.43	1.02	2066.08	45.21	0.00
	1500	500	0.43	1.03	2075.23	54.36	0.00
	1500	150	0.41	1.02	2079.46	58.59	0.00
	1000	50	0.44	1.03	2079.89	59.02	0.00
	1500	10	0.43	1.02	2084.54	63.67	0.00
	2000	25	0.45	1.02	2084.87	64.00	0.00
	1000	500	0.43	1.02	2085.71	64.84	0.00
	1000	250	0.41	1.02	2091.47	70.60	0.00
	1500	100	0.31	1.03	2096.33	75.46	0.00
	1000	25	0.43	1.02	2096.46	75.59	0.00
	1500	50	0.37	1.02	2108.23	87.36	0.00

1000	150	0.41	1.02	2128.74	107.87	0.00
1000	100	0.41	1.02	2136.63	115.76	0.00
1500	250	0.49	1.02	2174.09	153.22	0.00
1000	10	0.46	1.01	2202.90	182.03	0.00
NA	NA	0.39	1.03	2219.60	198.73	0.00

Table S3: Ecological threshold values for seven high conservation value species relative to LiDAR-derived measures of forest structure. Values represent the lower and upper bounds of the zone of transition, characterizing a state of rapid change in occurrence.

Species	Gap fraction	Number of canopy layers	Canopy height (m)	Plant area index	Structural diversity index	Shape
Banded civet	0.32-0.73	0.79-2.07	7.86-19.29	1.96-5.06	2.04-3.02	0.78-0.92
Binturong	-	-	8.57-22.14	-	1.73-2.71	-
Bornean yellow muntjac	-	-	6.43-18.57	1.63-4.41	1.86-2.71	-
Long-tailed porcupine	0.33-0.76	-	8.57-25.00	1.96-5.39	2.10-3.27	0.78-0.93
Marbled cat	-	-	-	1.80-4.90	-	-
Sambar deer	-	0.64-2.29	-	-	-	0.77-0.93
Sunda clouded leopard	0.31-0.73	-	8.57-21.43	1.96-4.90	1.73-2.78	-
Tufted ground squirrel	-	-	8.57-24.29	-	2.04-3.08	-

Table S4: Area (ha) and proportion of total forest cover in parentheses of conservation and restoration areas delineated by the prioritization framework. We partition cover by forest class to provide an indication of designations relative to a degradation gradient.

Forest Class	Conservation Areas	Restoration Areas
Forest Cover	11,323.28 (27.37)	16,410.32 (39.67)
Old Growth	1,684.28 (14.87)	1,664.84 (10.15)
Managed	7,899.36 (69.76)	5,612.96 (34.20)
Heavily-degraded	1,696.16 (14.98)	7,046.68 (42.94)
Remnant	42.92 (0.38)	2,086.40 (12.71)

Table S5: Area (ha) and proportion of total forest cover in parentheses of conservation and restoration areas delineated by the prioritization framework. We partition cover by forest class and the number of target species conserved within each forest class.

Forest Class	Number of target species	Conservation areas	Restoration areas
Forest Cover	1	2033.64 (17.96)	5363.72 (32.69)
	2	1268.48 (11.20)	3496.92 (21.31)
	3	1329.16 (11.74)	1874.32 (11.42)
	4	874.00 (7.72)	1041.80 (6.35)
	5	1953.04 (17.25)	911.44 (5.55)
	6	1673.96 (14.78)	663.32 (4.04)
	7	2191.00 (19.35)	3058.80 (18.64)
Old Growth	1	323.36 (19.20)	320.52 (19.25)
	2	162.76 (9.66)	326.00 (19.58)
	3	163.00 (9.68)	114.48 (6.88)
	4	117.00 (6.95)	122.68 (7.37)
	5	317.68 (18.86)	133.80 (8.04)
	6	157.20 (9.33)	194.96 (11.71)
	7	443.28 (26.32)	452.40 (27.17)

Managed	**1**	**729.08 (9.23)**	**2904.60 (51.75)**
	2	702.60 (8.89)	1456.28 (25.94)
	3	1048.92 (13.28)	404.24 (7.20)
	4	607.84 (7.69)	174.72 (3.11)
	5	1557.92 (19.72)	140.48 (2.50)
	6	1505.28 (19.06)	152.08 (2.71)
	7	1747.72 (22.12)	380.56 (6.78)
Heavily-degraded	1	946.92 (55.83)	941.84 (13.37)
	2	394.20 (23.24)	1467.60 (20.83)
	3	116.92 (6.89)	1209.32 (17.16)
	4	149.16 (8.79)	665.36 (9.44)
	5	77.48 (4.57)	484.20 (6.87)
	6	11.48 (0.68)	290.24 (4.12)
	7	0.00 (0.00)	1988.12 (28.21)
Remnant	1	34.40 (80.15)	1196.88 (57.37)
	2	8.20 (19.11)	247.12 (11.84)
	3	0.32 (0.75)	146.48 (7.02)
	4	0.00 (0.00)	79.16 (3.79)
	5	0.00 (0.00)	153.00 (7.33)
	6	0.00 (0.00)	26.04 (1.25)
	7	0.00 (0.00)	237.72 (11.39)

References

1. D. Harding, M. Lefsky, G. Parker, J. Blair, Laser altimeter canopy height profiles: methods and validation for closed-canopy, broadleaf forests. *Remote Sensing of Environment* **76**, 283-297 (2001).
2. S. C. Stark *et al.*, Amazon forest carbon dynamics predicted by profiles of canopy leaf area and light environment. *Ecology Letters* **15**, 1406-1414 (2012).
3. H. Tang *et al.*, Retrieval of vertical LAI profiles over tropical rain forests using waveform lidar at La Selva, Costa Rica. *Remote Sensing of Environment* **124**, 242-250 (2012).
4. R. H. MacArthur, H. S. Horn, Foliage profile by vertical measurements. *Ecology* **50**, 802-804 (1969).
5. T. Jucker *et al.*, Canopy structure and topography jointly constrain the microclimate of human-modified tropical landscapes. *Global Change Biology* **24**, 5243-5258 (2018).
6. J. R. Kellner, G. P. Asner, Convergent structural responses of tropical forests to diverse disturbance regimes. *Ecology letters* **12**, 887-897 (2009).
7. M. Plummer (2003) JAGS: A program for analysis of Bayesian graphical models using Gibbs sampling. in *Proceedings of the 3rd international workshop on distributed statistical computing* (Vienna, Austria).
8. A. Gelman, D. B. Rubin, Inference from iterative simulation using multiple sequences. *Statistical science* **7**, 457-472 (1992).

9. A. Gelman, X. L. Meng, H. Stern, Posterior predictive assessment of model fitness via realized discrepancies. *Statistica Sinica* **6**, 733-760 (1996).

10. G. Guillera-Arroita, Modelling of species distributions, range dynamics and communities under imperfect detection: advances, challenges and opportunities. *Ecography* **40**, 15 (2017).

11. D. I. MacKenzie *et al.*, *Occupancy estimation and modeling: inferring patterns and dynamics of species occurrence* (Elsevier, 2017).

12. J. F. Brodie *et al.*, Correlation and persistence of hunting and logging impacts on tropical rainforest mammals. *Conservation Biology* **29**, 110-121 (2015).

13. R. S. Mordecai, B. J. Mattsson, C. J. Tzilkowski, R. J. Cooper, Addressing challenges when studying mobile or episodic species: hierarchical Bayes estimation of occupancy and use. *Journal of Applied Ecology* **48**, 56-66 (2011).

14. J. E. Hines *et al.*, Tigers on trails: occupancy modeling for cluster sampling. *Ecological Applications* **20**, 1456-1466 (2010).

15. R. M. Dorazio, N. J. Gotelli, A. M. Ellison, "Modern methods of estimating biodiversity from presence-absence surveys" in Biodiversity loss in a changing planet. (InTech, 2011).

16. K. Pacifici, E. F. Zipkin, J. A. Collazo, J. I. Irizarry, A. DeWan, Guidelines for a priori grouping of species in hierarchical community models. *Ecology and Evolution* **4**, 877-888 (2014).

17. A. Gelman, Prior distributions for variance parameters in hierarchical models. *Bayesian Analysis* **1**, 515-533 (2006).

18. M. Kéry, M. Schaub, *Bayesian population analysis using WinBUGS: a hierarchical perspective* (Academic Press, 2011).

19. K. McGarigal, H. Y. Wan, K. A. Zeller, B. C. Timm, S. A. Cushman, Multi-scale habitat selection modeling: a review and outlook. *Landscape Ecology* **31**, 1161-1175 (2016).